1995

Thermohaline Structure of an Eddy-Resolving North Atlantic Model: The Influence of Boundary Conditions

John M. Klinck
Old Dominion University, jklinck@odu.edu

Original Publication Citation

Klinck, J.M. (1995). Thermohaline structure of an eddy-resolving North-Atlantic model - The influence of boundary-conditions. *Journal of Physical Oceanography, 25*(6), 1174-1195. doi: 10.1175/1520-0485(1995)0252.0.co;2

Thermohaline Structure of an Eddy-Resolving North Atlantic Model: The Influence of Boundary Conditions

JOHN M. KLINCK

Center for Coastal Physical Oceanography, Department of Oceanography, Old Dominion University, Norfolk, Virginia

(Manuscript received 13 July 1993, in final form 15 September 1994)

ABSTRACT

A T–S volumetric census, with a resolution of 0.2°C and 0.1 psu, for years 20–25 of the World Ocean Circulation Experiment Community Modeling Effort eddy-resolving simulation of the equatorial and North Atlantic Ocean, reveals how the thermohaline character of the model has changed from the initial conditions, which were taken from the Levitus climatology. Any changes in the thermohaline structure, other than stirring, mixing, or geostrophic adjustment of smoothed climatology, must be due to the boundary conditions, which are imposed at the surface and at four sponge layers (northern boundary, southern boundary, Labrador Sea and Mediterranean Sea), where water temperature and salinity are nudged toward climatological conditions.

Several unrealistic thermohaline features appear in the solution, which can be traced to these surface and lateral sponge boundary conditions. 1) Water masses from the Arctic Ocean are overrepresented in the model. The volume transport across the northern sponge is twice the value estimated from observations. The heat flux is approximately correct, while the salt flux is large by a factor of 4. 2) Water masses from the South Atlantic are underrepresented. The transport of water across the southern sponge is about two-thirds of the observed value, but the salt flux is comparable with estimates. However, the heat flux is only 10% of measured values due to a missing equatorward motion of warm surface waters. 3) Water masses from the Labrador Sea and Baffin Bay are overrepresented. The volume flux is twice that observed, while the heat flux from the sponge is realistic. The salt flux is about 20% of the observed value. 4) Finally, Mediterranean Water is underrepresented. Even though the volume transport across the sponge is eight times the observed value, the net salt flux is small by a factor of 400, leading to an insufficient production of salt.

All of these difficulties with the model T–S structure are traced to three general problems. First, the flow at the outer edge of the sponges is strongly barotropic in spite of the fact that the temperature and salinity fields are from climatology. Part of the problem with the sponges may be the smoothed nature of the climatology, which has the effect of reducing density gradients, thereby reducing geostrophic shears. In all cases, except the southern sponge, the volume transport across the sponge is two to eight times larger than the value expected from other analyses or observations. Since the vertical structure of the flow is set by the climatology, the only way to create this additional transport is through barotropic flow. The reason for the additional transport is not entirely clear, but it may be due to the excessive vertical velocities that are demanded by the conversion process in the sponges. These vertical motions create bound vortices in the sponge layers that drive recirculation in the vicinity of the sponges, increasing the transport without changing the heat or salt flux. The second problem is due to geometric effects within the sponges. One such problem is that Iceland blocks the exchange along the northern sponge. Another problem is that the ocean bathymetry is specified in the sponge layer. For example, the inner Mediterranean sponge is so shallow (around 100 m) that there is very little area in which to modify the water. Similar conditions occur in the Labrador sponge where the water is also 100 m deep. The third general problem is the use of relaxation to climatology to represent surface freshwater fluxes, which leads to unrealistic surface forcing if the currents are displaced from climatological locations. The combination of a displaced Gulf Stream and the relaxation of surface salinity to climatology produces mode waters that are unrealistically cool and fresh.

1. Introduction

Advances in the understanding of ocean circulation dynamics and the development of high capacity computing have made possible realistic simulations of oceanic flow. These simulations have advanced to the point that it is now possible to quantitatively compare simulated properties, such as temperature and salinity, to observed distributions or to climatologies. The Community Modeling Effort (CME), which was undertaken as part of the World Ocean Circulation Experiment (WOCE), was an attempt to produce the most realistic simulation of the north and equatorial Atlantic Ocean that was possible given 1) the current understanding of ocean processes, 2) the ability to include these processes in ocean circulation models, 3) the current ability to estimate external forcing on the ocean, and 4) the present computer capacity. However,

Corresponding author address: Dr. John M. Klinck, Center for Coastal Physical Oceanography, Old Dominion University, Crittenton Hall, Norfolk, VA 23529.

the success of such a realistic experiment can only be determined after the fact by a rigorous analysis of the model-derived fields. For the CME, several studies have been undertaken to assess how well the model solutions compare to actual ocean distributions. In particular, effort has been expended on the determination of which processes account for good agreement between simulations and observed fields and which result in poor agreement.

This study reports on a comparison between the simulated temperature and salinity and observed distributions. The comparisons are made using a standard volumetric census approach in which the volume of water having a particular range of temperature and salinity is calculated from the model. These volumes are then compared against similarly estimated volumes from an ocean climatology (Levitus 1982).

The intent of this analysis is to assess the structure of the simulated temperature and salinity, which will provide a measure of the realism of the thermohaline processes included in the CME simulation. This assessment is of particular importance because thermohaline forcing in the simulation occurs not only at the surface but also at four sponge layers (described below), which represent water conversion processes occurring in other regions of the ocean not explicitly included in the model.

Comparison of the simulated temperature and salinity with observed values allows a quantitative estimate of the type and amount of different water masses that are created at the surface and at the four boundary layers. If these regions create improper water masses or incorrect amounts of particular water masses, then the thermohaline structure of the model will change inexorably to an unrealistic state. Given the present-day emphasis on simulating oceanic circulation for global climate studies, it is important to determine how well basin- and global-scale models represent these oceanic processes.

The following section describes briefly the circulation model that was applied to the Atlantic Ocean. Some general descriptions of the analysis technique are also given. Section 3 presents the volumetric census used in this analysis and provides some detail on the estimation of boundary fluxes. The results of the volumetric census and flux analysis are presented in section 4 and discussed in section 5. The last section is a summary.

2. CME Model details

The model domain used for the CME covered the Atlantic Ocean from 15°S to 65°N [for a detailed description, see Bryan and Holland (1989)], which includes the equatorial current bands, the subtropical gyre, and parts of the polar gyre (Fig. 1). The northward boundary of the model occurs at the submarine ridge that stretches from Scotland to Iceland and on to

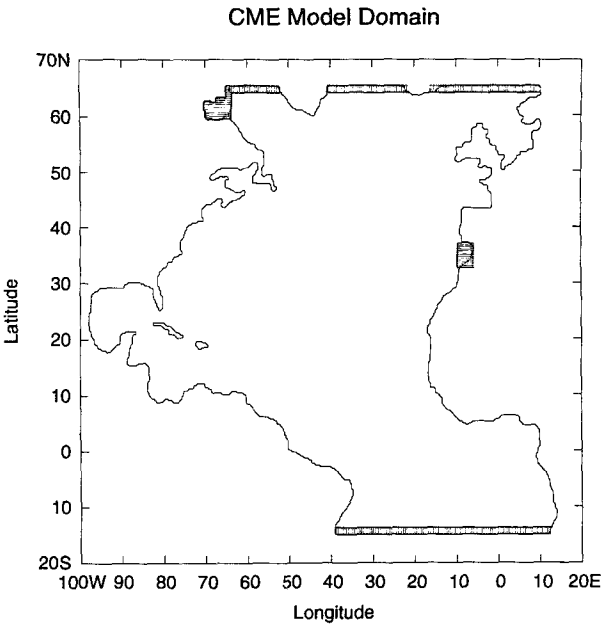

FIG. 1. Domain of the Community Modelling Effort Atlantic model. The solid lines are land boundaries and the hatched areas indicate the location and size of boundary zones in which temperature and salinity are nudged to climatological values.

Greenland. The size of the basin is dictated, to a large extent, by the available computer resources, but the choice of locations for the boundaries was made to exclude dynamically separate parts of the ocean (e.g., the water mass formation region in the Norwegian and Greenland Seas). Only the islands of Cuba and Hispañola are represented as true islands; other islands in the Atlantic are shallow banks that extend almost to the ocean surface.

The basic structure of the numerical model used for the CME simulation comes from the NOAA Geophysical Fluid Dynamics Laboratory (GFDL) numerical model, developed by Bryan (1969). This model uses second-order accurate finite differences on an Arakawa B-grid (Mesinger and Arakawa 1976) and is designed to conserve first and second moments (e.g., mass, heat, and energy) of the dependent variables in the model. A tracer, which represents the age of water parcels, was included. The value of the tracer is set to zero at the surface and increases linearly with time below the surface.

Model grid spacing is 1/3° latitude and 2/5° longitude, which yields a spatial resolution of about the local radius of deformation at midlatitudes, thus, allowing dynamical instabilities to form mesoscale eddies. The vertical structure of the flow is represented by up to 30 levels with a spacing of 35 m at the surface that increases smoothly to 250 m near middepths. The ocean depth at each point was extracted from a 5′ (latitude and longitude) gridded dataset without any general smoothing. Single point highs and lows were re-

moved, and the Florida channel was deepened slightly so that it will have the correct cross-sectional area.

Conservative choices were made for the representation of diffusion and viscosity. Specifically, horizontal subgrid-scale dissipation is biharmonic diffusion, with a coefficient of 2.5×10^{11} m^4 s^{-1}, for both momentum and the tracer. Vertical viscosity is Laplacian diffusion with a constant coefficient of 3×10^{-3} m^2 s^{-1}; diffusion of scalars (temperature, salinity, and age) is similarly represented with a coefficient of 3×10^{-5} m^2 s^{-1}. There is a separate mixed layer at the surface, and density convection occurs through a vertical-averaging scheme.

The simulation was started from rest with the initial temperature and salinity taken from the Levitus (1982) climatology. Surface wind stress and wind work were determined from the Hellerman and Rosenstein (1983) monthly climatology. Heat flux was obtained from a bulk formula (Han 1984) using estimated monthly atmospheric temperature. Freshwater flux was estimated indirectly by forcing (that is, nudging or Newtonian damping) the model surface salinity to the seasonal salinity (Levitus 1982) with a relaxation time of 50 days. All of the forcing is interpolated linearly to each model time step.

Because of the limited model domain, boundary conditions represent processes in the excluded parts of the ocean. To this end, there are four buffer zones (also called "sponge layers" or "sponges," Fig. 1), each having a width of six grid points in which the temperature and salinity of the water are nudged to values taken from the Levitus climatology. The nudging timescale in these buffer zones decreases from 25 days at the outer edge to 5 days at the inner part of the buffer. These boundary zones are not "open" in that there is no flux of water across the model boundary, rather these are conversion regions where the thermohaline properties of the water are changed.

The model simulation was run for 25 years and conditions during the last 5 years are in an approximate statistical steady state. There are several analyses of the simulation starting with a general description (Bryan and Holland 1989) of the steady circulation, temperature structure, and thermohaline overturning cell. Additionally, there are estimates of the transport of the Florida Current, the northward heat flux (every 3 days through the year), and root-mean-square displacement of the free surface (estimated from the pressure distribution under the rigid lid). One important result from this analysis is that the northward heat flux due to mesoscale eddies is negligible compared to that due to advection. The eddy energy was sufficiently low that a second simulation with reduced dissipation parameters (reduced by 2.5 for biharmonic parameters and by 3.0 for vertical parameters) was calculated starting at year 20 and continuing for 5 years. This simulation had improved, but still low, energy levels.

An analysis of the kinetic energy budget (Treguier 1992) reveals that kinetic energy is approximately correct in the western half of the Atlantic Ocean, while that in the eastern side is low by about an order of magnitude. The basic conclusion of this study is that the processes that give rise to the variability are present in this eddy-resolving, primitive equation model but the viscosity is too large (i.e., the solution is not inertial enough) to allow an adequate transfer of energy to the mesoscale eddies.

The southeastern edge of the subtropical gyre (Canary Basin) has been analyzed for the influence of the Mediterranean outflow (Spall 1990). In addition to the previously mentioned low eddy kinetic energy, this study finds that the influence of the Mediterranean Water is inadequate. However, the general structure of the flow is in agreement with observations, and analysis of the solution has lead to some additional mechanisms to create the observed flow variability. A second study on the variability of the Cape Verde front (Spall 1992) considers the effect of Rossby wave radiation on the eddy energy levels in the eastern basin of the Atlantic Ocean. Stability analysis and observations show this region to be a source of internal Rossby wave energy.

Finally, the circulation in the equatorial Atlantic has been analyzed (Schott and Böning 1991) to consider the effect of reducing the influence of vertical friction. Some features are well represented (retroflection of the North Brazil Current into the North Equatorial Countercurrent) while others are not (insufficient penetration of the Equatorial Undercurrent, persistent meanders in the retroflection). The simulation with smaller dissipation parameters has a more realistic circulation.

3. Analysis

One way to characterize the thermohaline state of the ocean is to calculate the volume of water between certain values of temperature and salinity. Worthington (1981) is an example of a finescale analysis where the water classes are defined by temperature and salinity intervals of 0.1°C and 0.01 psu. This census used all of the acceptable observations, so it is not possible to analyze changes in the T–S structure of the ocean over time (interannual or seasonal).

A volumetric T–S census is a good way to analyze the solution of a numerical model because it is a bulk measure (independent of spatial variability) of internal conversion processes (mixing and convective adjustment) as well as boundary forces (surface and sponge fluxes). The analysis is much easier in a numerical model since the thermohaline structure of the solution is known, and a volumetric census can be calculated, at every time step. Furthermore, the gridding of the model partitions the ocean into convenient volumes, in contrast to estimating volumes from hydrographic observations. Finally, the census can be done on each saved model state or on a time average of the model with equal ease.

a. Volumetric T–S census of water masses

All of the analyses in this paper consider water mass classes that are defined by differences of 0.2°C and 0.1 psu for temperature and salinity. The range of values for salinity is 29.0–38.1 psu (90 classes) and for temperature it is −5.0° to 32.0°C (185 classes). Although this is not as fine as the Worthington (1981) census, it is adequate to represent the major types of water found in the Atlantic. There has been no attempt at this time to split the census geographically, for example, by latitude bands, although it is possible to do so [for examples of this sort of analysis, see the unreviewed article, Klinck (1994)].

Observational studies convert in-situ temperature to potential temperature to remove effects of compression so that observations from different depths can be compared. The circulation model used for the CME calculation, however, includes the assumption that water is incompressible, which gives rise to the equation of conservation of volume as a governing equation. Thus, the model dynamics are constrained such that there is no temperature change due to a pressure change. Essentially, the variable in the numerical model called temperature is, in fact, potential temperature. Throughout the paper, this model variable will be called temperature (and designated by T) rather than potential temperature (which is usually designated θ).

The grid boxes in the model range in size depending on location. The thinnest box (near the surface) has a thickness of 35 m while the thickest (near the bottom) is 250 m thick. All of the grid boxes are 37.06 km (1/3° lat) in meridional extent and the zonal distance (2/5° long) is 44.47 km at the equator and decreases as the cosine of the latitude to a minimum of 18.8 km at the northern end of the model. The largest volume for a grid box is obtained at the deepest level on the equator (412 km^3) and the smallest volume is at the surface on the northern edge of the model (24 km^3). The results of this study are presented as the $\log_{10}$ of the volume of water (in km^3), so the smallest grid box has a value greater than 1.0, which represents the resolution of the volumetric census.

b. T–S analysis of boundary fluxes

The thermohaline state of the model is forced by imposed fluxes at the ocean surface and by water mass conversion in the four sponge layers. The surface forcing is specified as a boundary condition for the model, so these fluxes are well known. The sponge layers also force the model: the nature of this forcing is not controlled externally but is determined by the velocity and density in the vicinity of the sponges during the course of the simulation.

Since the lateral diffusive fluxes in the model are small (Bryan and Holland 1989), it is possible to estimate the effect of the sponge boundary regions by calculating the advection of water into and out of the sponge by T–S class. Specifically, a boundary plane, coincident with the temperature and salinity grid points, is defined six grid intervals from the model boundary. This plane is partitioned by the model grid into rectangles having values of temperature and salinity in the center, thus, defining the T–S class for the rectangle. The velocity is known at the edges of the rectangle on either side (horizontally) of temperature and salinity values, so the average of the normal component of velocity characterizes the flow across the boundary.

For each of the sponge boundaries, the flux, defined as the area of the grid box times the average normal flow, is accumulated for each T–S class separately for positive and negative flow. The exchange is presented as two figures showing the transport (displayed as the $\log_{10}$ in units of $m^3\ s^{-1}$) by T–S class in each direction relative to the sponge. The total volume flux along with net heat and salt change for each of the sponges for the 5-year average of the model solution is also calculated.

c. Thermohaline steadiness in years 20–25

The temperature and salinity climatology created by Levitus (1982) is taken to represent the present state of the ocean. Using it as the initial condition means that the model ocean begins with a thermohaline structure very close to present-day conditions. However, during the initial stages of the simulation, the model converts some of the potential energy of this initial density field into kinetic energy through the process of geostrophic adjustment. Because of the dominance of potential energy in the ocean over kinetic, there is a very small reduction of the potential energy. However, all of the property gradients are made tighter since the geostrophic flow has horizontal gradients governed by the internal radius of deformation (15–30 km) and the climatology has been smoothed to length scales of several degrees of latitude and longitude. Geostrophic adjustment does not, in itself, modify the volumetric T–S character of the model.

However, the sharper lateral gradients increase the diffusive flux, which will cause some modification of the temperature and salinity structure. Since lateral mixing is represented as a biharmonic process, it is very weak on scales of several hundred kilometers. A more active mixing process is vertical mixing, which is made stronger by the increasing slope of the property surfaces that occurs during geostrophic adjustment.

Once the model density gradients and velocity shears reach a critical level, then mesoscale eddies develop through dynamical instabilities. These eddies have spatial scales of one to two hundred kilometers and will stir the ocean, increasing the magnitude of the diffusive flux of heat and salt.

By model year 20, most of the adjustment of the model to the initial conditions has occurred. The analysis below shows that the changes in the temperature

and salinity over 5 years (model years 20–25) repeat with a seasonal cycle, and the anomaly from this seasonal cycle is small and has no drift that is detectable above the variability. Therefore, averaging the model over these 5 years is meaningful, and the volumes of different T–S classes will be stable. Any drift in the thermohaline character of the model cannot be detected in any reliable way by simply taking a difference of two model states but must instead be analyzed by considering the details of the changes in the volumetric census from the initial conditions.

The T–S volumetric census described above is calculated on each of the model states saved at 3-day intervals over the last 5 years of the simulation. These volumes can be used to estimate the net heat and salt flux from the surface and the four sponges. The amount of water that is changing from one T–S class to another is also calculated. The time variability of these processes over the last 5 years of the simulation will indicate the approximate steadiness of the thermohaline structure.

The first diagnostic is the volume of water that changes from one T–S class to another. This calculation is made by taking the difference of consecutive volume censuses and then separately adding the positive and negative changes. Since there is no change in the total volume of the ocean, the absolute value of these sums is the same. A 5-year time series is thereby constructed of the net volume of water changing its T–S state. The time series is split into segments representing each year and these five 1-year series are averaged to get an annual cycle in thermohaline volume change for the simulation (Fig. 2a). About 10^9 m^3 of water (out of a model volume of 1.88×10^{17} m^3) change from one T–S class to another in any 3-day interval in the model. There is a seasonal cycle with the largest changes occurring in winter and summer, which is expected as these are the times of the largest surface heating and cooling. The anomaly from this seasonal cycle (Fig. 2b) is a few percent of the average change and displays no long-term trend. Thus, the total amount of water changing T–S classes is essentially steady over the last 5 years of the model run.

The second diagnostic is the total heat required to change the calculated volume of water between temperature classes. That is, a certain amount of heat is required or released as water moves from one T–S cell to another over the 3-day period. The sum of all of these heat changes is the total heat that the model absorbed through the five boundaries. Note that the total heat flux in the model may be larger than the sum that is calculated here as some parts of the ocean can give up heat to other parts and these internal transfers will cancel out in this calculation. Net heat flux is calculated between each model saved state to give a 5-year time series. This is averaged as described above to give an annual-average net heat flux for the model (Fig. 3a). The average net heat flux has an amplitude of about 4.0 petawatt with warming in the summer and cooling in the winter. The variations from this annual pattern (Fig. 3b) have an amplitude less than 10% of the maximum and again show no distinct trend.

The third diagnostic is the total salt required to change the calculated volume of water between salinity classes. As in the case with heat for the temperature changes, salt is absorbed or released in changing the volume of water between salinity classes. The total of all of these changes gives the net salt flux from the boundaries. The resulting 5-year time series is averaged to give the annual cycle of salt flux (Fig. 4a). Salt is added to the model in the late winter and spring with a maximum rate of 2.0×10^6 kg of salt per second while the loss of salt occurs at about half that rate for a longer time. The variability of the salt flux from the annual pattern (Fig. 4b) is much different from the other two diagnostics, having an amplitude almost as large as the seasonal cycle and having very high frequency changes. Nevertheless, in spite of the larger variability of the salinity flux, there is no long-term trend over the last 5 model years.

These three analyses of time evolution of the temperature and salinity structure of the last 5 years of the simulation lead to the conclusion that a regular seasonal cycle has been set up in the model and that there is no long-term trend in these changes that can be detected over this 5 years of model history. There is, in fact, a slow drift in the thermohaline state of the model, which can not be detected from these bulk diagnostics but instead is indicated by changes in the volumes of certain water types. The sections below indicate the changes that occur and present reasons why these changes are occurring.

4. Results

Two general results are presented in this section: volumetric census by temperature and salinity classes and volumetric flux by temperature and salinity class at the sponge boundaries. The T–S census of the Levitus climatology is presented first and described in order to see water masses that are present at the beginning of the simulation. The focus will be on water masses created at the surface (subtropical and subpolar mode waters) and in the various sponges (Arctic and Labrador Sea waters, Mediterranean Water, and South Atlantic and Antarctic waters). The T–S census has been calculated from the average of the last 5 years of the model simulation. The difference between the Levitus and model T–S censuses indicates how the model thermohaline structure has changed from the initial state. A small part of the change will be due to the adjustment of the model to initial conditions and some initial mixing. This adjustment will lead to some smoothing to the thermohaline distributions in the model but will not cause the changes indicated below.

The 5-year mean model solution is used to calculate the volume flux of water by temperature and salinity

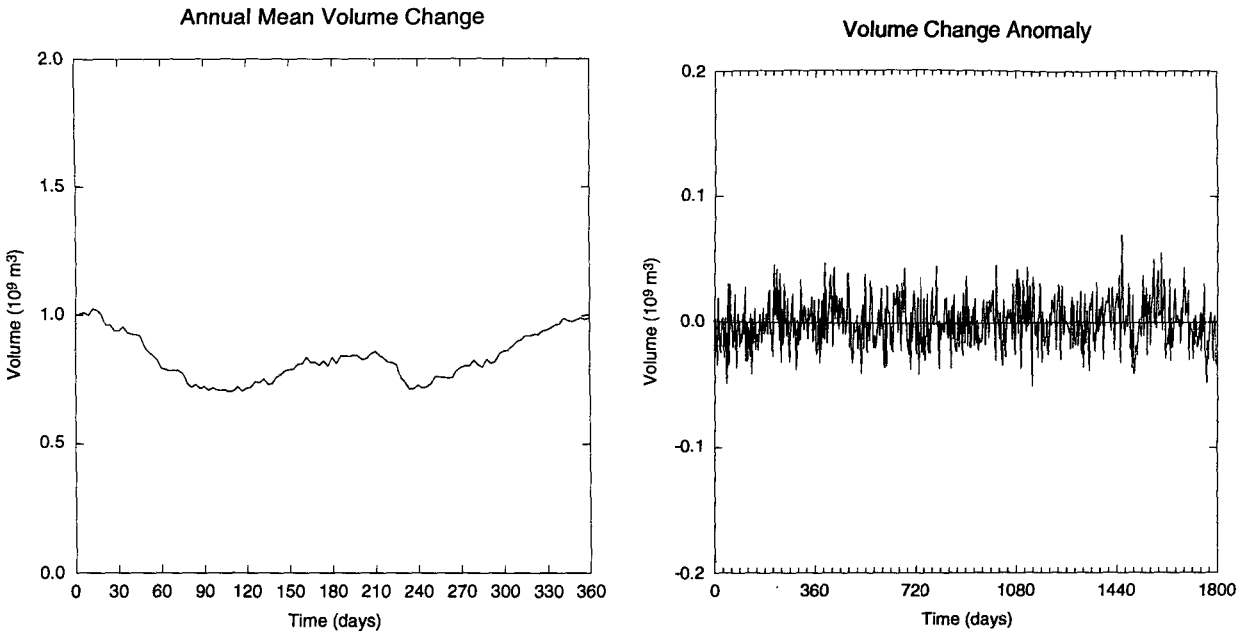

FIG. 2. Volume of water changing temperature or salinity between two successive model saved states (3-day interval). This volume was calculated from the difference of the volume of each temperature and salinity class from two successive save states and then separately summing the positive and negative volume changes. (a) Annual average change for the last 5 years of the model solution. (b) Anomaly of volume change from the annual average change over the last 5 years of the model solution.

class across the outer boundary of each of the four sponge boundary layers. The calculation separately accumulates the volume of water moving across the boundary in each direction so that inflow and outflow can be analyzed. Net fluxes of heat and salt are then calculated for the sponge as a whole.

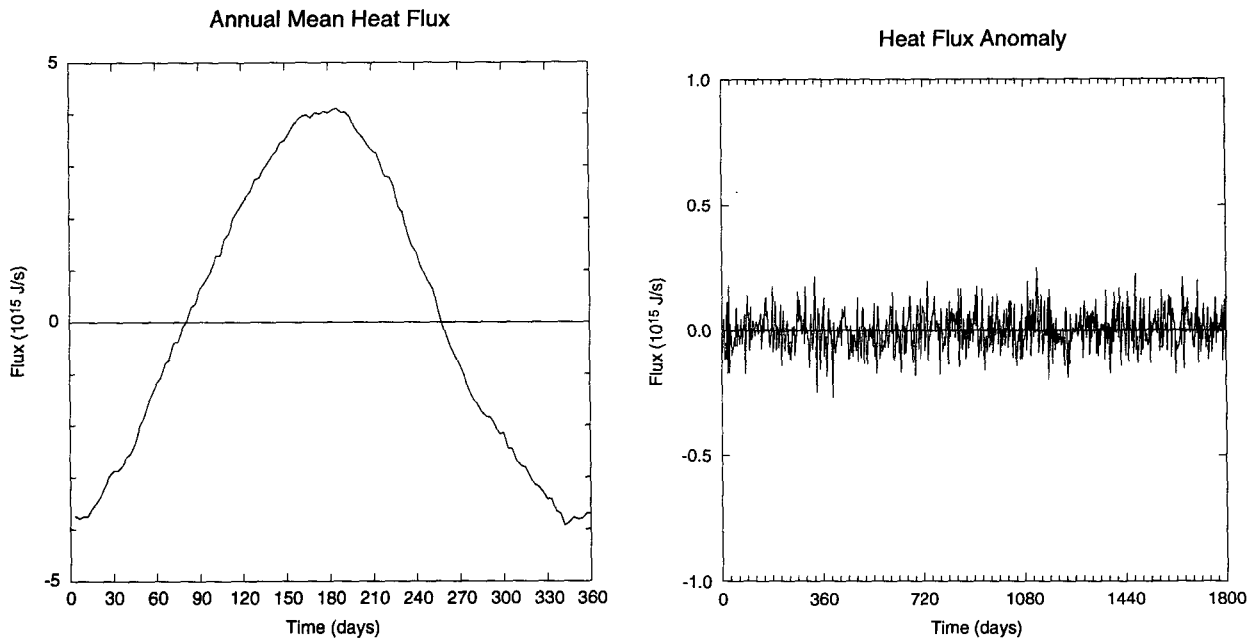

FIG. 3. Total heat flux required for the calculated temperature change in the model between successive model states (3-day interval). This heat flux is provided by surface flux and by four sponge boundary layers. (a) Annual average flux for the last 5 years of the model solution. (b) Anomaly of heat flux from the annual average over the last 5 years of the model solution.

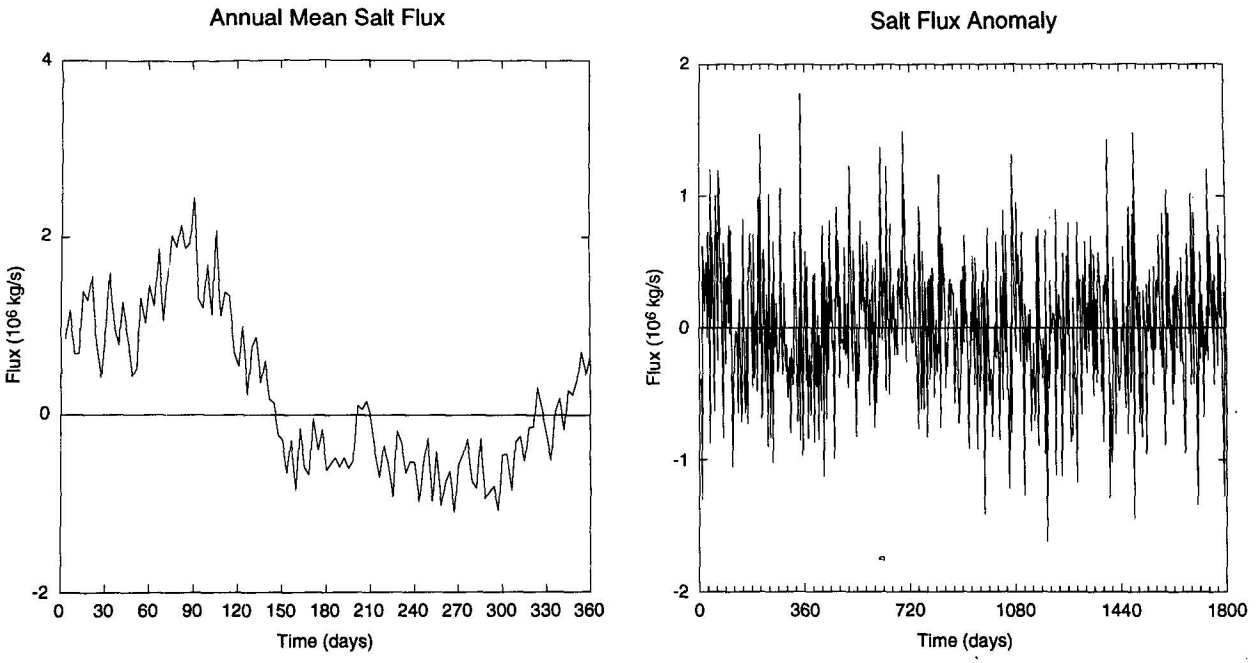

FIG. 4. Total salt flux required for the calculated salinity change in the model between successive model states (3-day intervals). This salt flux is provided by surface flux and by four sponge boundary layers. (a) Annual average flux for the last 5 years of the model solution. (b) Anomaly of salt flux from the annual average over the last 5 years of the model solution.

a. Census of the Levitus climatology

A volumetric *T–S* census of the Levitus (1982) climatology for the North and equatorial Atlantic (Fig. 5), covering the same ocean area as the model domain, identifies the water masses that should exist. These water masses come from a variety of regions and are created by a number of processes, so it will be possible to use over- or underabundances to indicate the realism of various model processes. Table 1 lists water masses that exist in the census of the Levitus climatology. There is some variation in the definition of water masses, and in some cases, water masses are lumped into general classes (e.g., Arctic waters and North Atlantic Deep Water) when there are actually several distinct classes that can be identified, usually by salinity differences of few thousands of a part per thousand, which are not resolved by this census, or by differences in dissolved oxygen or nutrient concentration.

It is useful, at this point, to identify some of the classes of water that appear so that later differences will be clearer. At the warmest end of the diagram are warm and salty waters from low latitudes, an example of which is Subtropical Underwater (25°C, 36.8 psu: Wüst 1964), which is found at the upper-right end of the *T–S* diagram (Fig. 5). These waters are due to surface forcing (warming and evaporation). Next are several types of subtropical mode water, created by annual winter cooling. These are generally termed North Atlantic Central Water (on a line between 8°C, 35.1 psu and 19°C, 36.7 psu), although there is a persistent mode known as 18°C Water (Worthington 1959; Warren 1972). A similar range of subtropical mode water exists in the southern Atlantic, the South Atlantic

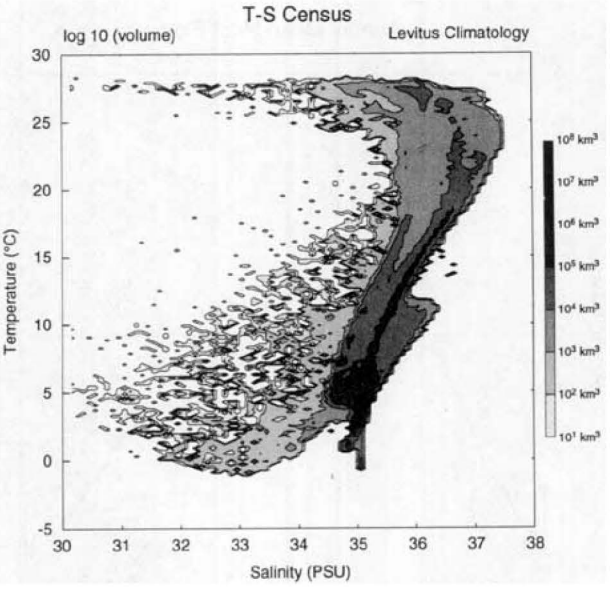

FIG. 5. Volumetric census by temperature and salinity class of the climatology constructed by Levitus (1982). Values are shown as the log base 10 of the volume in km^3. The resolution of the census is 0.2°C and 0.1 psu. The contour interval is 1.0, which represents an order of magnitude change in the volume. Darker shading indicates larger volumes as shown by the scale bar.

TABLE 1. Water types and masses used in this paper are defined by name and by ranges of temperature and salinity. Each definition is followed by a reference for the values used. The entry labeled "N. Atlantic to Arctic" is the character of the water near the surface that enters the Arctic from the North Atlantic.

Name	Temperature (°C)	Salinity (psu)	Reference
		Water types	
Mediterranean	12	36.5	Tchernia (1980)
Antarctic Intermediate	4	34.4	Tchernia (1980)
		Water masses	
Subtropical Underwater	25	36.8	Wüst (1964)
18° Water	18	36.5	Worthington (1959)
Subpolar mode	10–15	35.5–35.6	McCartney and Talley (1982)
Mediterranean	8–9	35.7	Tchernia (1980)
N. Atlantic to Arctic	6–9	35.3	Swift (1986)
Subpolar mode (Lab. Sea)	4.0–4.5	34.95–35.0	McCartney and Talley (1982)
Labrador Sea (winter)	3.0–3.5	34.88–34.94	Tchernia (1980)
Antarctic Intermediate	3–5	34.7–34.9	Tchernia (1980)
N. Atlantic Deep	2.3–3.5	34.90–34.98	Tchernia (1980)
Arctic (generic)	0–3.0	34.9	Swift (1986)
Antarctic Bottom	.1	34.67	Tchernia (1980)
Norwegian Sea	−1.0	34.91	Tchernia (1980)
Baffin Bay surface	−1.0–5.0	30.0–33.5	Tchernia (1980)
Baffin Bay Winter	−1.6	<33.8	Tchernia (1980)
		Extended water masses *T–S* point to *T–S* point	
N. Atlantic Central	8, 35.1	19, 36.7	Tchernia (1980)
S. Atlantic Central	6, 34.5	19, 36.0	Tchernia (1980)

Central Water, which is about 0.5 psu fresher than the corresponding water mass in the North Atlantic.

The Mediterranean outflow produces a warm and salty water type, the exact definition of which depends on the distance from the strait at which the water is being defined. During the cascade from the Strait of Gibralter to depths of 1000 m or so, Mediterranean Water mixes with surrounding Atlantic water to produce a parent water type at 12°C and 36.5 psu (Tchernia 1980). This water continues to spread at midlevels in the North Atlantic, resulting in a large volume of water at 8°–9°C and 35.7 psu (Tchernia 1980).

Colder waters are produced at polar latitudes and move equatorward in the interior and at the bottom of the ocean. Several types of subpolar mode water come from the Labrador Sea (McCartney and Talley 1982), which produces water masses above 1000 m with temperatures of 3.0°–4.5°C and salinity from 34.88 to 35.0 psu. The Norwegian–Greenland Sea produces a relatively salty deep water that slips over the ridge between Greenland and Scotland to become North Atlantic Deep Water (2.3°–3.5°C and 34.90–34.98 psu (Tchernia 1980).

Two influences from the Southern Hemisphere are also apparent in the census. Antarctic Intermediate Water (3°–5°C and 34.7–34.9 psu) (Tchernia 1980), a form of subpolar mode water, is visible in the southern end of the model domain as water at 1000-m depth along the east coast of South America. This water mass erodes by mixing as it progresses to the north. Antarctic Bottom Water (0.1°C and 34.67 psu) (Tchernia 1980) is also evident, although this water mass also looses its character by mixing as it flows northward.

b. Census of 5-year mean solution

The volumetric census of the model solution (Fig. 6) averaged over the last 5 years, model years 20 through 25, is used to analyze the difference between the Levitus and model solutions. However, there are several general observations that can be made about this census.

The most obvious change is the spread of the model census to fresher values; that is, the envelope of observed *T–S* classes has moved left and up in the diagram (Fig. 6). One possible explanation is that there is more vertical mixing in the model, so there is a tendency to fill the area between the warm and fresh surface waters and the deeper central waters. The other explanation is that the surface forcing is creating fresher mode waters, which fill this region of *T–S* space. In particular, there is a fresh and cool mode water (Fig. 6) extending from 12°C, 33 psu to 17°C, 35 psu.

A second general observation is that there is water colder than −1.8°C, which would be frozen in the ocean. Although the amount of this anomalously cold

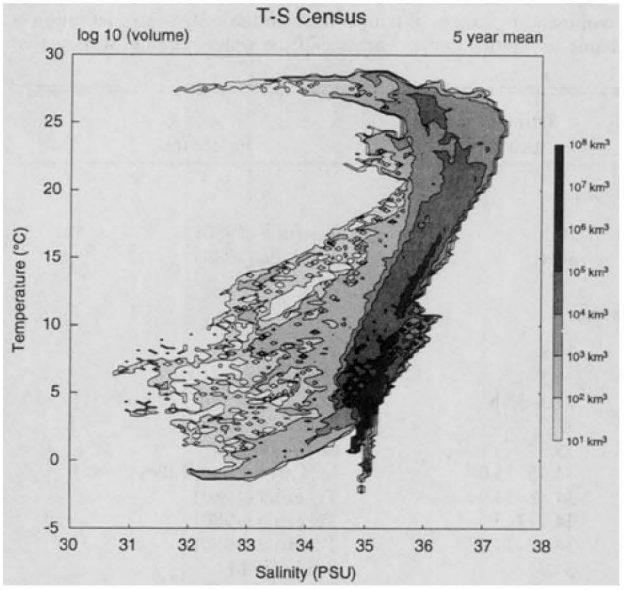

FIG. 6. Volumetric census by temperature and salinity class of the average of the last 5 years of the model calculation. Values are given as the log base 10 of the volume in cubic kilometers. The resolution of the census is 0.2°C and 0.1 psu. The contour interval is 1.0, which represents an order of magnitude change in the volume. Darker shading indicates larger volumes as shown by the scale bar.

water (a dozen or so model cells) is small, one wonders what would have happened if the water were to freeze. The simplest answer is that all of this water would be limited in how cold it could get, so the T–S volumes would simply occur at −1.8°C; that is, the pendulous parts near the bottom of the volumetric diagram would be pushed upward to the freezing point. However, the freezing of this water would release salt, but where this salt would go is not obvious.

One might wonder how subfreezing water can occur in this simulation, but the explanation is straightforward—there is no mechanism in the model to create ice (there is no ice submodel). The equation of state used in the model produces a value for the density of water with temperatures below the freezing point so the model does not suffer any ill effects. The model is unaware, and unconcerned, that there is subfreezing water, and so the simulation proceeds. The surface cooling, therefore, produces subfreezing water, which is dense and is mixed into the interior by the convective mixing scheme. In the ocean, the water would freeze and only salt would be mixed into the interior. The effect of such misrepresentation of processes in the model is not evident, but no wildly unrealistic situations occur as a result.

c. *Differences between Levitus and the mean solution*

The difference between these two censuses are made clearer by subtracting the Levitus (1982) census from the 5-year average model census and showing the results as the excess (Fig. 7a) and the deficit (Fig. 7b) of the model volume relative to Levitus. The differences between the two calculations are shown as the percent change from the Levitus values.

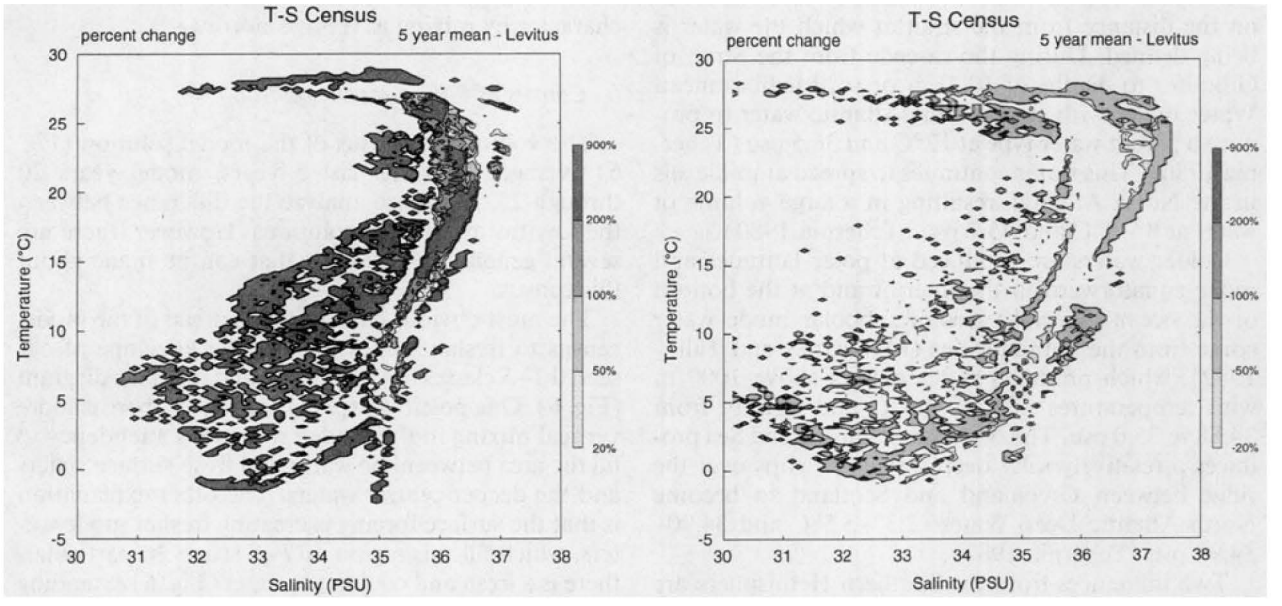

FIG. 7. The difference (model minus Levitus) between the previous volumetric censuses. The resolution of the census is 0.2°C and 0.1 psu. Darker shading represents a larger percentage change as indicated by the scale bar. (a) Positive differences between the two censuses. There is more water in these classes in the model than in the climatology. (b) Negative differences between the two censuses. There is less water in these classes in the model than in the climatology.

TABLE 2. Flux of volume, heat, and salt from the four sponge boundary regions. The volume flux is the amount of water crossing the outer edge of the sponge in one direction only. There is an equivalent transport in the other direction to conserve mass. The heat and salt fluxes are net fluxes and the direction is indicated by the compass direction in parenthesis. The last two columns are the average temperature or salinity change that would result from the given fluxes across the boundary. The temperature change is calculated by dividing the net heat flux by the volume flux, the base density (1028 kg m^{-3}), and the specific heat (3.8×10^3 J kg^{-1} $°C^{-1}$). The salt change is obtained by dividing the salt flux by the volume flux and the base density.

Boundary	Volume flux (Sv)	Heat flux (J s^{-1})	Salt flux (kg s^{-1})	ΔT (°C)	ΔS (PSU)
North	28.0	$+2.0 \times 10^{14}$ (N)	$+3.1 \times 10^7$ (N)	−1.80	−1.00
South	21.0	$+1.2 \times 10^{13}$ (N)	$+1.6 \times 10^7$ (N)	+1.40	+0.73
Labrador	9.3	-2.0×10^{13} (W)	-1.8×10^6 (W)	−0.55	−0.19
Mediterranean	8.5	-2.7×10^{12} (W)	-8.8×10^4 (W)	+0.90	+0.10

There is an excess of water in the model solution (Fig. 7a) at several places in T–S space. The surface waters warmer than 27°C are overrepresented in the model solution as are mode waters around 35.5 psu and above 20°C. In the model, there is an overabundance of North Atlantic Central Water, although at the warmer end of this water type it appears that the model subtropical mode water is fresher than the comparable type in Levitus. A wide variety of water fresher than 34.5 psu and warmer than 5°C appear in the model that do not exist in the ocean. There is a very lumpy representation of North Atlantic Deep Water or polar mode water (colder than 9°C and near 35 psu) and an excess of Arctic water colder than 1°C and near 35.0 psu. Finally, subfreezing water exists between 32.0 and 34.5 psu and also at 35 psu.

The model is deficient in several water masses. There is too little water at all salinities between 26° and 28°C. Most of the warm water (greater than 16°C) that is saltier than 36.5 psu is missing from the solution. Almost all of the South Atlantic Central Water and the Mediterranean influences are absent. Much of the water cooler than 2°C and fresher than 34.5 psu is missing. A volume of water near 1°C and 34.8 psu is missing.

These results can be summarized by considering masses of water that are missing, displaced, or unrealistic. Much of the warm salty water (say, the Subtropical Underwater) has been made fresher by the model. Equatorial surface water is about 1°C too warm. Similarly, the warmer end of North Atlantic Central Water is too fresh in the model. On the other hand, both South Atlantic Central Water and Mediterranean Water do not appear in the model with appropriate volumes. The water between 3° and 10°C centered on 34.8 psu are not well mixed since adjacent T–S classes are either over- or underrepresented. Much of the subfreezing water seems to have been created from water at the same salinity but with temperatures between 0° and 2°C. Finally, the missing water near 1°C and 34.8 psu, given the low salinity, seems to be due to insufficient influence of Antarctic Bottom Water. These differences between the censuses will be reconsidered after estimating the flux of different water classes across the boundary sponges.

d. Fluxes of water by T–S class from boundary sponges

The sponge boundary layers at four places in the model (Fig. 1) provide a significant influence on the thermohaline structure. Since the horizontal diffusive and eddy fluxes across these boundaries are weak (Bryan and Holland 1989), the major influence is the advection of water across the outer boundary of the sponge and the conversion of this water from one T–S class to another by nudging in the interior of the sponge. The volume flux (m^3 s^{-1}) across the outer edge of these sponge layers for each temperature–salinity class was calculated. The sign convention on the fluxes is that a positive flux is in the direction of positive flow normal to the boundary, rather than being into or outward from the model volume. That is, a positive flux at the northern sponge is to the north (out of the model), while a positive flux at the southern sponge is also to the north (into the model). For each of these flux calculations, three quantities are considered (volume flux, net heat flux, and net salt flux) with the values given in Table 2. The net heat and salt flux are the sum of all fluxes from the boundary and represent a net influence of the sponge. The net volume flux from each sponge is zero because of the conservation of volume in the model. However, the sum of all of the fluxes in one direction indicates the amount of water being processed by the sponge and this number is given in Table 2 as the volume flux for the sponge.

As a further bulk diagnostic, the flux-weighted temperature and salinity change is also calculated for each sponge to indicate the overall change being produced by the sponge region. For example, it is expected that the northern sponge will make water colder and the Mediterranean sponge will make it saltier. The bulk diagnostics in Table 2 will help quantify these changes.

The volume flux by T–S class at the northern sponge is given as northward flux (Fig. 8a) and southward flux (Fig. 8b). In general, the sponge takes in water that is between 4.0° and 8.0°C and around 35.0 psu and returns to the model water that is about 5.0°C and 34.8 psu. This change agrees with the general perception that the Arctic mainly cools the relatively warm, salty

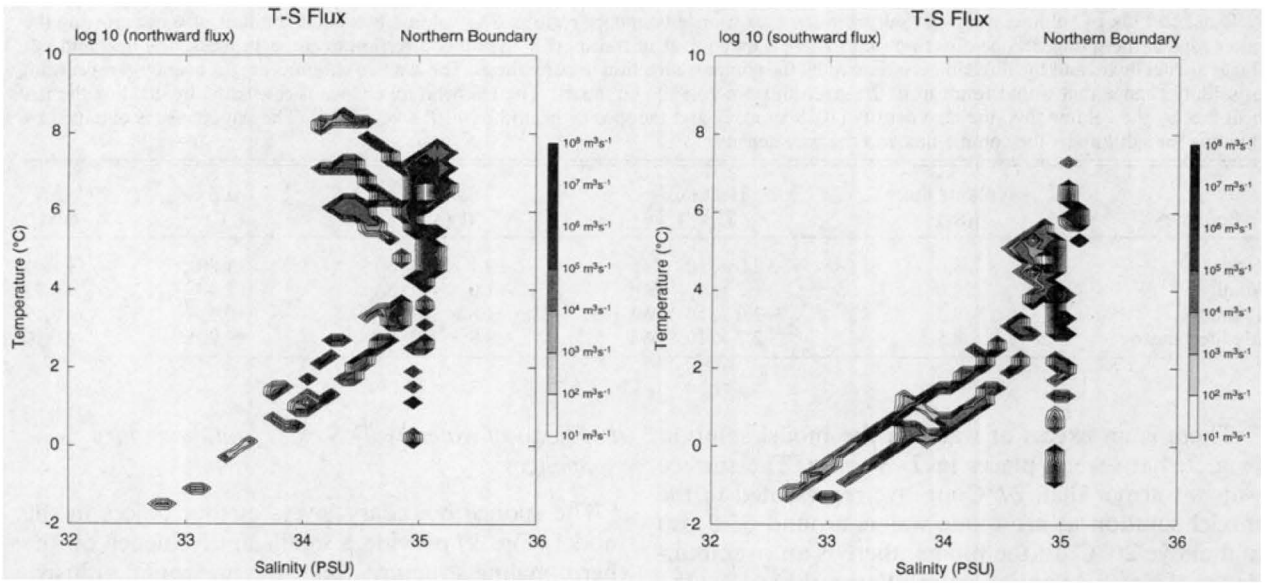

FIG. 8. Flux of water ($m^3 s^{-1}$) across the outer boundary of the northern sponge layer by temperature and salinity class. A positive flux is northward (into the boundary). The contour interval is 1.0 and darker shading indicates larger flux. (a) Log base 10 of the positive part of the flux (into the boundary). (b) Log base 10 of the negative part of the flux (out of the boundary).

near-surface water from the North Atlantic. There is a second, lesser, inflow of water around 2.0°–3.0°C and 34.6 psu and a production of relatively fresh and cold waters around 34.0 ± 0.5 psu that is colder than 1.0°C. Note that there is significant recycling of water in these various classes. That is, even though water of a certain *T*–*S* class is produced by the sponge, there is a tendency for the boundary to pull water of a nearby *T*–*S* class into the sponge.

The locations where these transfers occur are best seen from the normal velocity, salinity, and temperature distributions at the outer edge of the sponge (Figs. 9a,b,c). The flow normal to the sponge (Fig. 9a) is strongly barotropic and horizontally banded. There is a general tendency for inflow to occur on the eastern side of the gaps and outflow to occur on the western side, but there is considerable variability from this basic pattern. Note that the sponge is blocked by Iceland (Fig. 1), so water that flows into the Norwegian Sea from the North Atlantic must exit the sponge on the eastern side of Iceland and reenter the sponge (perhaps) west of Iceland. This path is contrary to the normal route for water around the north side of Iceland where it is cooled and emerges at the Denmark Strait. The variability of the flow is not due to eddy effects, but rather due to persistant flow across the sponge boundary, which can be seen in the flow vectors (e.g., layer 3, which is at a depth of 91.6 m; figure not shown). The circulation in this region averaged over the winter months of the last 5 years is nearly identical with the flow averaged over all months in the last 5 years (figure not shown), which also argues against eddy effects.

Salinity (Fig. 9b) has little variation across this region with most of the water being near 35.0 psu, which is expected. Higher salinity occurs on the far western end of the section near the surface; lower salinity occurs along the east coast of Greenland (the East Greenland Current) and in the Labrador Sea (discharge from Baffin Bay). Most of the surface water on the eastern side of this section is above 5.0°C, while the surface waters on the western side are colder than 2°C (Fig. 9c). The deep water in the Norwegian Sea is colder than 1°C and there is some indication that this water is flowing over the sill at 10°W (recall that the Iceland–Faroe Ridge cuts diagonally across this latitudinal section).

The distribution of fluxes by *T*–*S* classes (Fig. 8a,b) comes from the structure of the flow at the outer edge of the sponge (Fig. 9a) and not from the distribution of temperature or salinity (Fig. 9b,c), which is being controlled by the Levitus climatology.

The southern boundary of the model crosses the tropical South Atlantic Ocean and, thus, represents the influence of the remainder of the World Ocean. The flux of water by *T*–*S* class (Fig. 10a,b) illustrates the various waters that are absorbed and created by this sponge. The northward flux (Fig. 10a) is the water ejected from the sponge. These water types are the warm and salty Subtropical Underwater and the South Atlantic Central Water, which is the broad water type stretching diagonally across the figure. At the cold end of the diagram, there is water at 34.8 psu centered on 2°C, which is Antarctic Bottom Water that has been modified by mixing as it crossed the South Atlantic. The sponge absorbs three main water masses that exist in the model (Fig. 10b). These are waters warmer than 24°C that are lower salinity surface waters from the equatorial band, a water mass between 16° and 20°C at around 35.6 psu, and North Atlantic Deep Water,

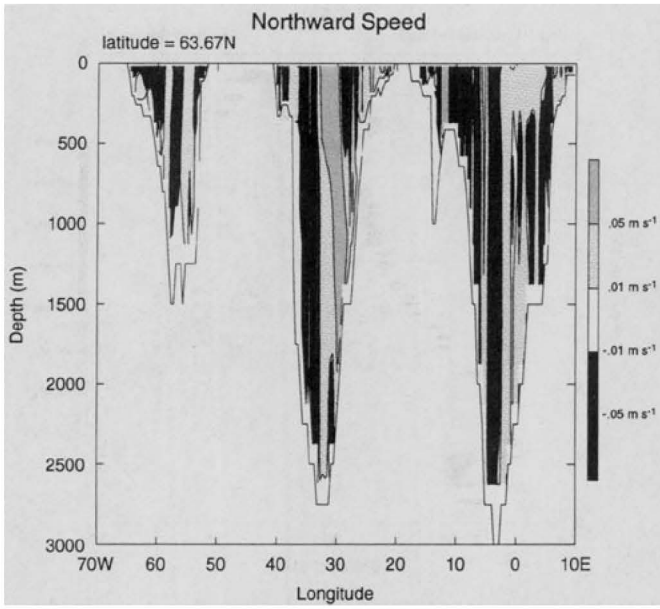

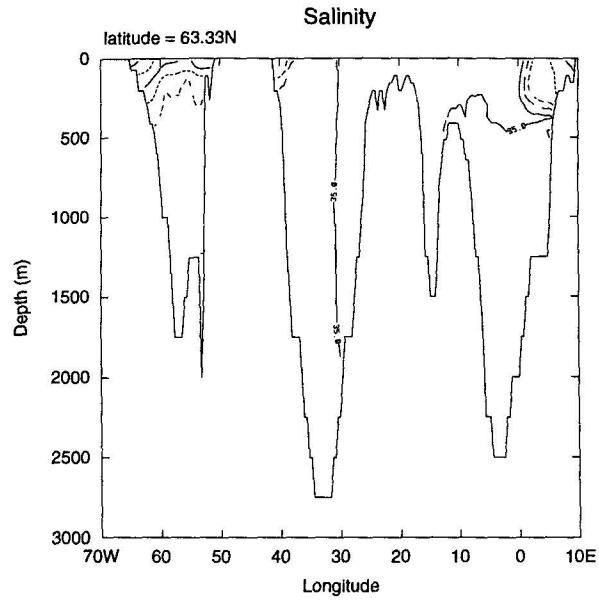

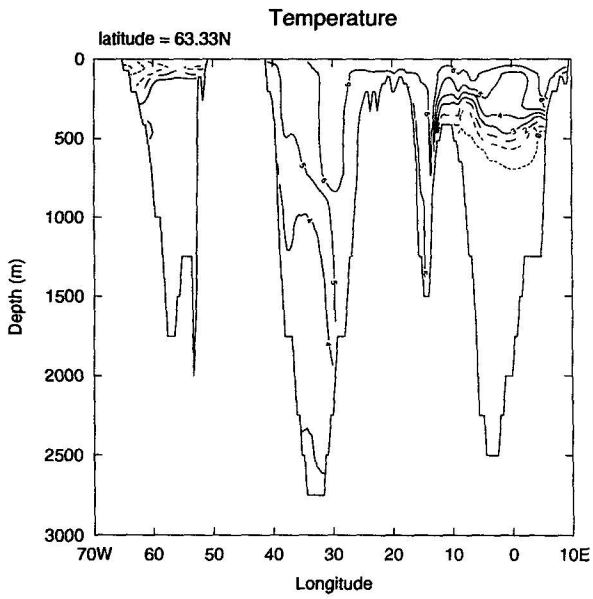

FIG. 9. Properties at the outer edge of the northern sponge. (a) Flow speed normal to the northern boundary at the edge of the sponge layer. The lighter gray shades indicate positive flow (into the boundary), while the darker shades indicate negative flow (out of the boundary). The speed ranges are indicated by the scale. (b) Salinity at the edge of the northern boundary sponge. The solid contour is 35.0 psu, while the dashed contours are 34.9, 34.8, and 34.5 psu for the long, medium, and short dashes, respectively. (c) Temperature at the edge of the northern boundary sponge. The contour interval is 1.0°C. Some contours are dashed with different patterns for better visibility.

which as part of the thermohaline overturning cell, is being exported to the Southern Ocean.

The velocity normal to the outer edge of the sponge (Fig. 11a) has a broad lateral structure above about 500 m and is alternating in direction below that depth. There is generally northward flow in the upper part of the western and central parts of the section, which is evident in the *T–S* flux as the northward motion of the South Atlantic Central Water. There is a general southward motion at the eastern end of the section, which is water from the Equatorial Undercurrent (16°–20°C) that has turned southward along the coast of Africa. The near-surface flow vectors (figure not shown) reveals three major features. In the far west, the flow at the edge of the sponge is mainly westward, and there is a strong recirculating gyre in the sponge (this is the southern subtropical gyre, which has been jammed into the sponge). The northward flow around 10°W is a persistent current that proceeds to the equator. This flow is water that comes from part of the Agulhas that turn into the Atlantic (this may be the South Equatorial Current or the Benguela Current), which is part of the warm path of the global thermohaline overturning cell. The southward flow along the coast of Africa comes from the equator (Angola Current).

The salinity structure (Fig. 11b) has higher salinity surface waters and lower salinity Antarctic Bottom

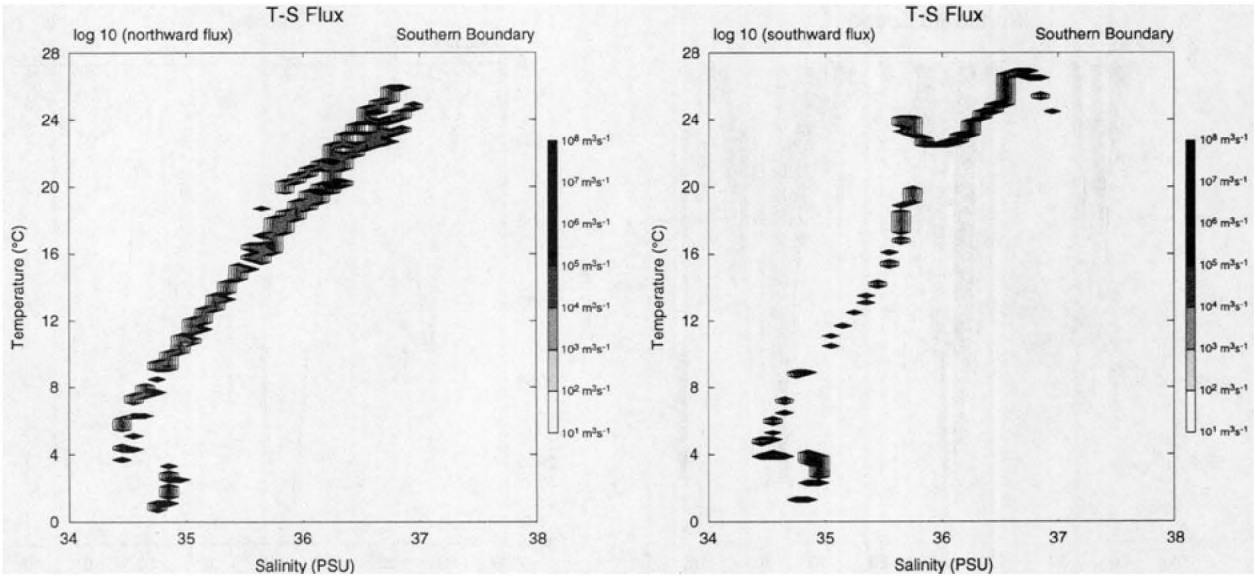

FIG. 10. Flux of water ($m^3 s^{-1}$) across the outer boundary of the southern sponge layer by temperature and salinity class. A positive flux is northward (out of the boundary). The contour interval is 1.0 and darker shading indicates larger flux. (a) Log base 10 of the positive part of the flux (out of the boundary). (b) Log base 10 of the negative part of the flux (into the boundary).

Water in the western basin. Antarctic Intermediate Water is evident as the salinity minimum along the western boundary. The temperature (Fig. 11c) structure at the southern sponge is reasonable, showing a tilt of the near-surface isotherms (upward to the east) due to the westerly wind forcing at the equator and the generally colder water in the deep western basin, due to the influence of Antarctic Bottom Water.

The sponge layer in the northwestern corner of the model represents the effects of the Labrador Sea and Baffin Bay, which should produce cold, relatively fresh water. The influence of this sponge layer is confused somewhat because the northern sponge overlaps the Labrador sponge (actually, the forcing region is "L" shaped and the zonal part of the sponge is called "northern" and the meridional part is called "Labrador"). The flux of water across the Labrador sponge (Fig. 12a,b) is mainly of Arctic character being 33.0 to 35.0 psu with temperatures between −0.5° and 5°C. However, the strongest volume flux into the sponge (Fig. 12b) is around 4°C and 34.9 psu and the strongest outflow (Fig. 12a) is about 0°C and 33–33.5 psu, characteristic of Baffin Bay water.

The normal velocity at the outer edge of the sponge (Fig. 13a) reveals the flow to be mainly barotropic with bands of alternating direction. The major inflows are in the center (61°N) and along the northern end of the section (64°N) and the major outflow is along the southern end of the section (60.5°N), which is appropriate for water created in the Labrador Sea and Baffin Bay region. The subsurface flow in this region (figure not shown) is generally along the sponge toward the south, leading to the formation of the Labrador Current. The salinity structure at the outer edge of the sponge (Fig. 13b) has freshwater at the surface that increases to 34.8 psu at 600 m. The coldest water (colder than 0°C) in the section (Fig. 13c) is along the northern side.

The flux of water by T–S class at the outer edge of the Mediterranean sponge has an unexpectedly wide distribution. The water flowing into the sponge (Fig. 14a) displays the same range of values as North Atlantic Central Water but exists as discrete, disconnected T–S classes. The outflow from the sponge (Fig. 14b) is spread over a similar range of values and is a little saltier than the inflow. There is a relatively large outflow class at around 11°C and 35.7 psu, which is approximately correct for Mediterranean Water. However, there are clearly a number of recirculations where water from the Atlantic is absorbed by the sponge and ejected with slightly changed characteristics.

The circulation across the outer edge of the sponge (Fig. 15a) is confined to the upper half of the water column and does not have the two-layered circulation that might be expected. Note, however, that this boundary is a considerable distance from the Strait of Gibralter. The strongest outflow is on the southern side of the section with speed 0.02 m s^{-1}. There is a general, but weak (less than 0.01 m s^{-1}), inflow along the center of the section. There are weak, deep outflows on either side of the section at about the correct depth for Mediterranean Water. The salinity (Fig. 15b) is highest at the surface and there is an interior salinity maximum along the Iberian coast at about 1000 m. The temperature distribution (Fig. 15c) is vertically layered without much lateral structure, although there is a ther-

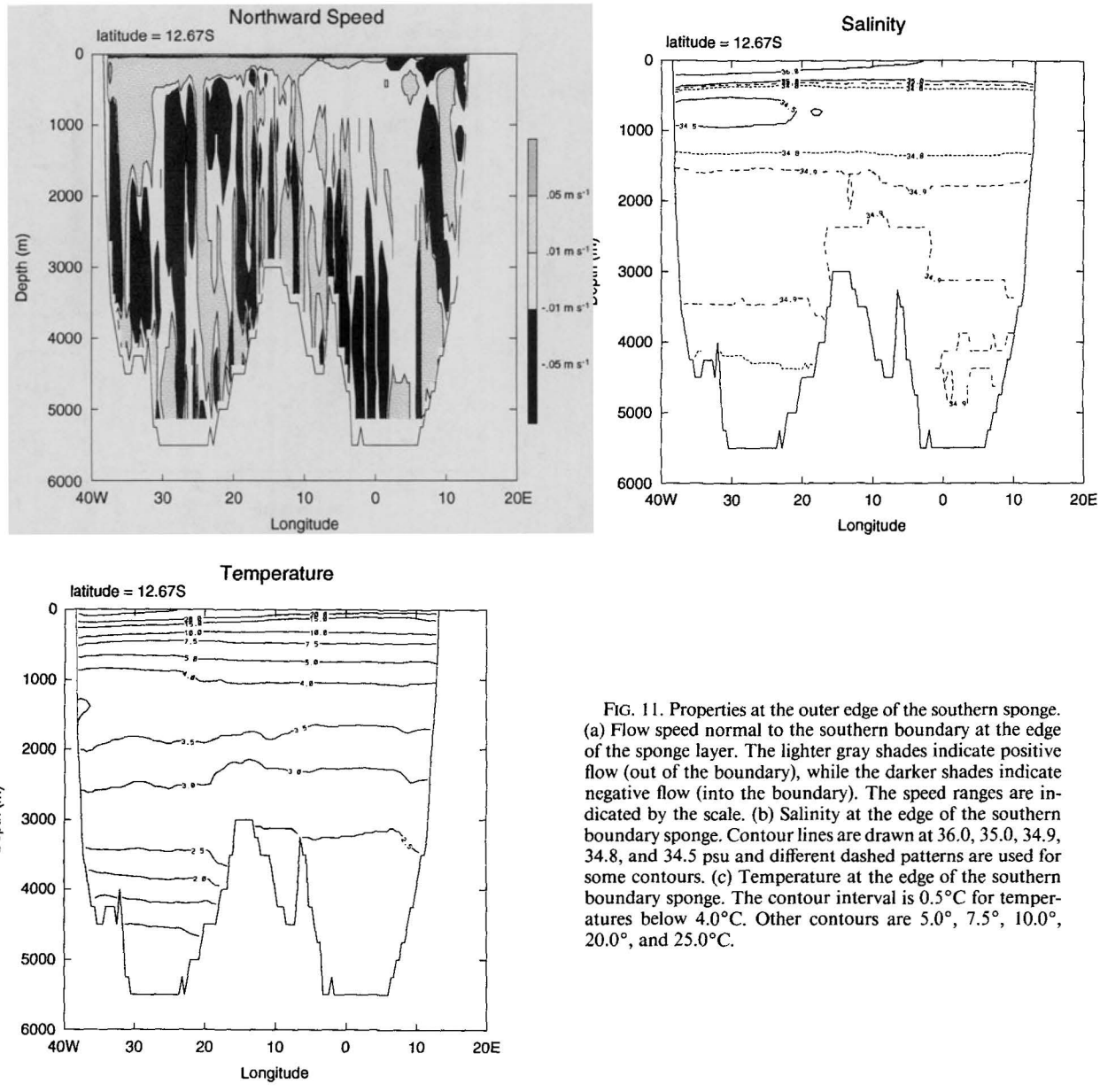

FIG. 11. Properties at the outer edge of the southern sponge. (a) Flow speed normal to the southern boundary at the edge of the sponge layer. The lighter gray shades indicate positive flow (out of the boundary), while the darker shades indicate negative flow (into the boundary). The speed ranges are indicated by the scale. (b) Salinity at the edge of the southern boundary sponge. Contour lines are drawn at 36.0, 35.0, 34.9, 34.8, and 34.5 psu and different dashed patterns are used for some contours. (c) Temperature at the edge of the southern boundary sponge. The contour interval is 0.5°C for temperatures below 4.0°C. Other contours are 5.0°, 7.5°, 10.0°, 20.0°, and 25.0°C.

mostad at around 800 m. The warm, salty outflow from the Mediterranean is occurring in two streams that hug the north and south walls of the embayment. However, the outflow along the northern wall is well above the salinity maximum, indicating a smaller salt transport than might have been expected. The sponge is also creating the Canary Current along the coast of Africa.

5. Discussion

The thermal and saline structure of the ocean is an integrated measure of internal and boundary processes. Since there are no internal sources or sinks of salt or heat, then the only internal influence is mixing and stirring, which tries to homogenize the water. Therefore, all of the thermohaline character of the ocean is determined by processes at the boundaries. In the CME model, there are five influential boundaries: the surface and the four sponge boundary layers. The influence of each of these boundaries on the volumetric T–S census is discussed in the following sections. The integrated effect of the sponge boundary layers is indicated in Table 2, which contains the volume flux in one direction across the sponge boundary along with the net heat and salt fluxes for each of the sponges. Also included is an average temperature and salinity change for the sponge, which is a general way to characterize the net effect of the sponge.

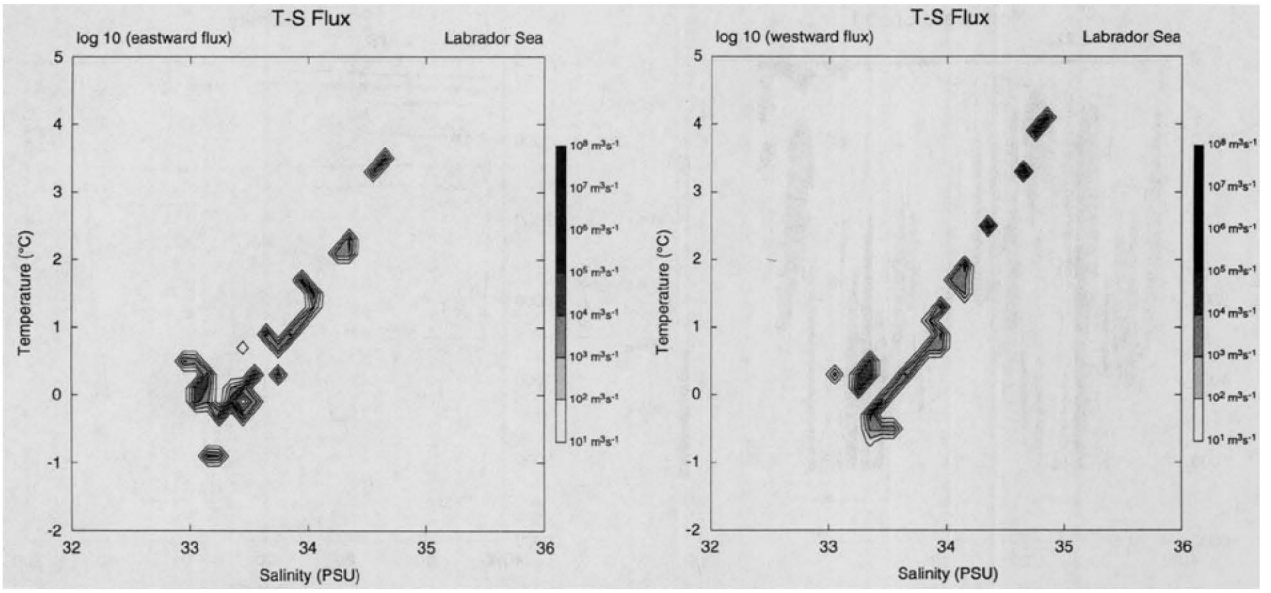

FIG. 12. Flux of water ($m^3\ s^{-1}$) across the outer boundary of the Labrador Sea sponge layer by temperature and salinity class. A positive flux is westward (out of the boundary). The contour interval is 1.0 and darker shading indicates larger flux. (a) Log base 10 of the positive part of the flux (out of the boundary). (b) Log base 10 of the negative part of the flux (into the boundary).

A general comment is that there is a tendency for the T–S census from the model (Fig. 6) to have less detail than the Levitus census (Fig. 5). In particular, the model has created water masses in the center of the diagram (10°–20°C and 32–35 psu). Part of this change in the census may be simply mixing of the detail that was originally present in the Levitus census. Another explanation is that several cool and fresh mode waters are being created by the model.

a. Surface influences

The surface layer of the CME model solution is affected by the surface heat flux and the relaxation of the surface salinity to climatological values in combination with convective adjustment. These influences have the strongest effect on mode waters, created by convection during winter cooling and on waters produced by excess evaporation. The difference in the T–S census for the model as compared to the Levitus census (Fig. 7a,b) indicates whether these processes are properly represented.

It is clear that the warm surface waters of the model are too fresh. The warmest waters with salinity above 36 psu are missing (Fig. 7b) while the corresponding waters between 35.5 and 36.0 psu are overabundant (Fig. 7a). The only mechanism to accomplish this is the salinity relaxation condition at the surface, which is freshening the surface layers of the model. Further evidence of the excess freshening is the tendency of the model to produce a census that spreads toward warmer and fresher waters. The surface heat flux may be incorrect also since the warmest waters in the model (near 28°C) are about one degree too warm (Fig. 7a).

Surface water at midlatitudes is being made fresher because the Gulf Stream does not separate at the proper latitude (near Cape Hatteras) but instead remains on the western boundary until Cape Cod. While seeming to be a small error, the interaction with the surface boundary condition is significant. The waters of the Gulf Stream are warmer and saltier than those north of the current. Therefore, the model Gulf Stream carries this salty water to a location where the surface salinity climatology expects to find fresher water. The surface relaxation then tries to make the water fresher, in effect causing a large precipitation estimated to be about 8 m of annual rainfall (F. Bryan, personal communication).

As an indicator of this influence, there are two unrealistic mode waters that are produced. These can be seen as an excess of volume (Fig. 7a) along two lines: 13°C, 33 psu to 16°C, 35 psu and 8°C, 33 psu to 12°C, 34.5 psu. The formation region of these water types is evident from the surface temperature and salinity (not shown). The same surface temperature distribution is obtained from both the 5-year average of the model solution and the average of all of the winter months. The only difference between these distributions is that the winter temperature along the Canadian coast (Labrador Sea) is below 1°C in winter and is around 4°C in the 5-year average. The only place where the above combination of temperature and salinity occurs is between the Gulf Stream and the United States–Canadian coast in a region roughly from 43° to 55°N, 60° to 45°W. This is also the region where the model Gulf Stream is most displaced from its proper position. The very strong freshening from the relaxation bound-

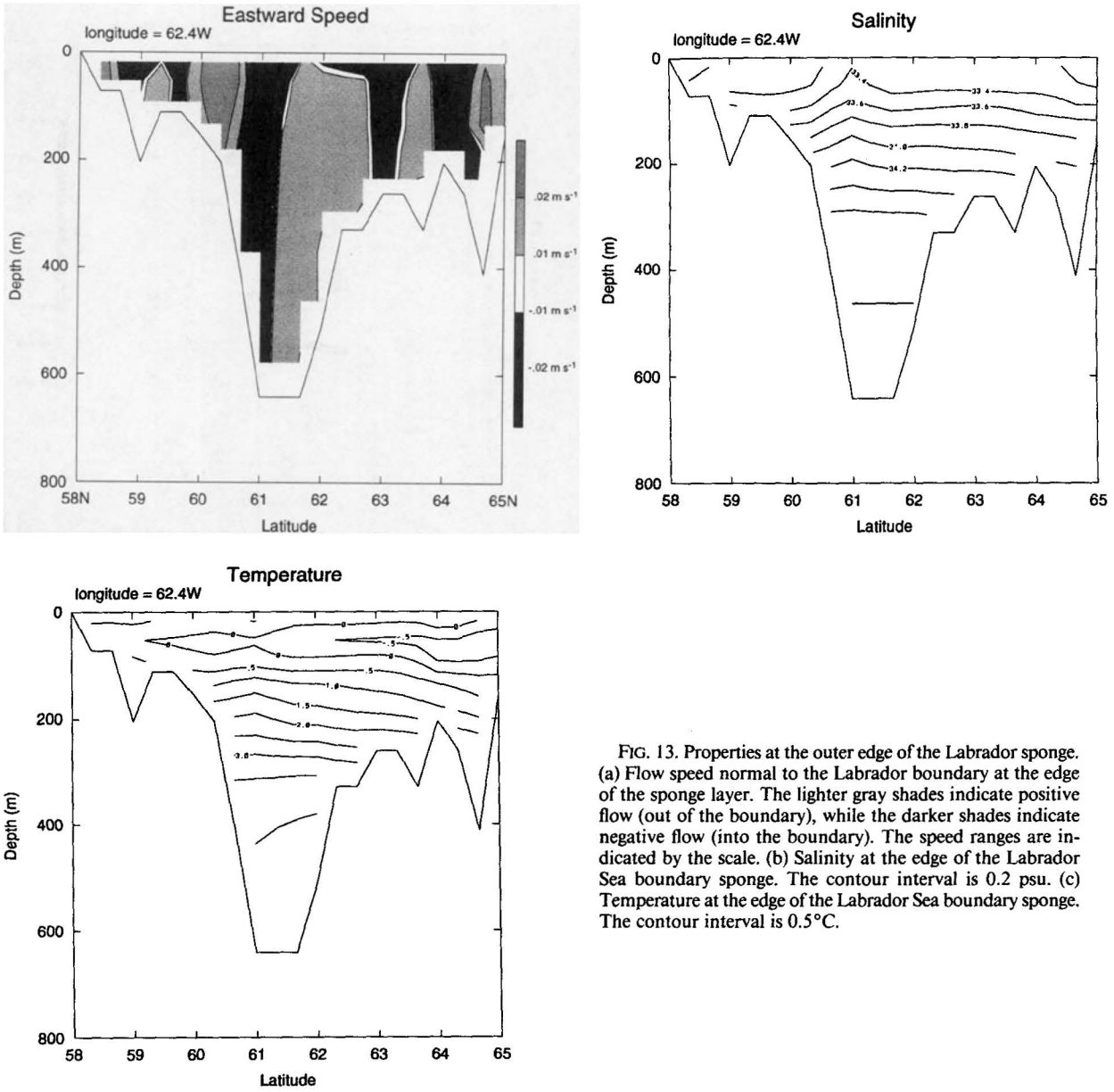

FIG. 13. Properties at the outer edge of the Labrador sponge. (a) Flow speed normal to the Labrador boundary at the edge of the sponge layer. The lighter gray shades indicate positive flow (out of the boundary), while the darker shades indicate negative flow (into the boundary). The speed ranges are indicated by the scale. (b) Salinity at the edge of the Labrador Sea boundary sponge. The contour interval is 0.2 psu. (c) Temperature at the edge of the Labrador Sea boundary sponge. The contour interval is 0.5°C.

ary condition coupled with cooling is creating the anomalous water masses.

b. Northern influences

The northern sponge layer exchanges about 28×10^6 $m^3\ s^{-1}$ of water and has the net effect of cooling the water by 1.8°C and freshening it by 1 psu (Table 2). The cooling is clearly appropriate as the Arctic Ocean is expected to produce cold, dense water. The freshening might be unexpected but it also is appropriate as it represents the influence of the East Greenland Current and the water from Baffin Bay, both of which are fresher than the North Atlantic contribution to the Arctic.

The total volume exchange at the northern sponge is high by a factor of 2 compared to a variety of estimates. Worthington (1981) estimated an exchange of 9×10^6 $m^3\ s^{-1}$ with two-thirds of the amount coming from the spilling of water over the Greenland–Iceland Ridge and the remaining third coming from the East Greenland Current. A later analysis (McCartney and Talley 1984), which considered explicitly the heat exchange between the Atlantic and Arctic, estimated the exchange to be 13×10^6 $m^3\ s^{-1}$. From direct current measurements, Dickson et al. (1990) observed 10.7

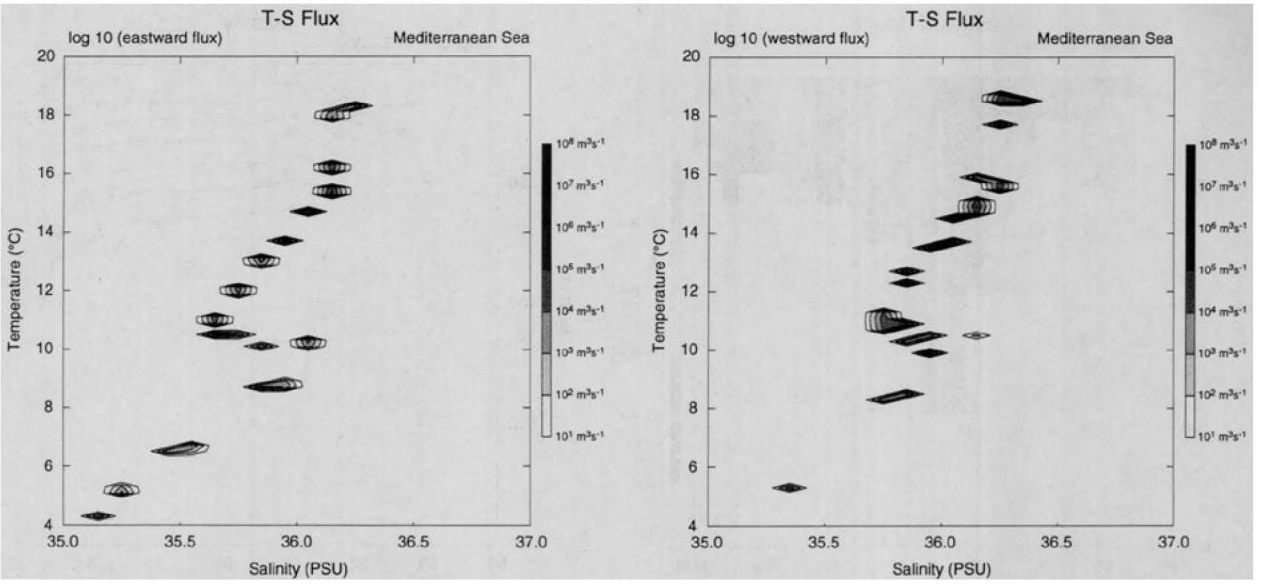

FIG. 14. Flux of water ($m^3 s^{-1}$) across the outer boundary of the Mediterranean Sea sponge layer by temperature and salinity class. A positive flux is westward (into the boundary). The contour interval is 1.0, and darker shading indicates larger flux. (a) Log base 10 of the positive part of the flux (into the boundary). (b) Log base 10 of the negative part of the flux (out of the boundary).

$\times 10^6$ $m^3 s^{-1}$ of flow into the North Atlantic (water with density greater than 27.8). Using estimates of thermohaline exchange in the North Atlantic, Speer and Tziperman (1992) calculated that 14.1×10^6 $m^3 s^{-1}$ of warm water moved from the Atlantic to the Arctic to be converted to denser waters for eventual return to the south. The model flux is about twice the magnitude of these estimates.

Estimates of the heat flux over the Arctic are relatively close: Hastenrath (1982) calculates 2.6 to 2.8 ($\times 10^{14}$ J s^{-1}), while Hsiung (1985) reports 1.8 to 2.6 ($\times 10^{14}$ J s^{-1}). By comparison, the model yields a heat flux of 2.0×10^{14} J s^{-1}. Furthermore, McCartney and Talley (1984) calculate a freshwater flux to the Norwegian Sea (0.035×10^6 $m^3 s^{-1}$) and the subpolar North Atlantic (0.188×10^6 $m^3 s^{-1}$), which translate to 1.26×10^6 kg salt s^{-1} and 6.76×10^6 kg salt s^{-1}, respectively, at 35.0 psu. This yields a total salt flux of 8.0×10^6 kg salt s^{-1}. The salt flux at the northern boundary in the model is about four times this value (Table 2).

The exchange of heat at the northern boundary is approximately correct, while the salt flux is about four times larger than the values calculated from observations. Since the temperature and salinity structure in the sponge is set by climatology, the reason for the enhanced exchange must be due to the circulation pattern. The normal flow at the edge of the sponge layer is strongly barotropic and alternating north and south. The climatological flow in this region is well known, but both the bandedness and lack of vertical structure seem unrealistic. A consideration of the flow from the model (figures not shown) indicates that the banded structure is due to large-scale currents that flow to and from the sponge and not small eddies at the edge of the sponge. In particular, the North Atlantic Current enters the sponge on the western side of Iceland rather than the eastern side. Since Iceland blocks the sponge, this current cannot enter the Norwegian Sea on the eastern side of Iceland and return to the North Atlantic on the western side.

c. *Southern influences*

The southern sponge exchanges about 21×10^6 $m^3 s^{-1}$ (Table 2), which is about two-thirds of the amount estimated to occur at 25°S (Tchernia 1980, p. 161). The sponge warms the water by 1.4°C and increases the salinity by 0.73 psu. These changes represent three major conversions: production of South Atlantic Central Water, Antarctic Intermediate Water, and Antarctic Bottom Water. Both of the Antarctic waters would be produced by cooling in the sponge, but the Central Water is produced by warming. The net warming is due to the larger volume of near-surface water produced relative to the Antarctic waters [23×10^6 $m^3 s^{-1}$ versus 12×10^6 $m^3 s^{-1}$ as estimated by Tchernia (1980)].

The heat flux across the subtropical South Atlantic is estimated to be northward with magnitudes of 8.3 $\times 10^{14}$ J s^{-1} (Fu 1981), 7.3 to 8.6 ($\times 10^{14}$ J s^{-1}) (Hastenrath 1982), and 1.98 to 8.6 ($\times 10^{14}$ J s^{-1}) (Hsiung 1985). The freshwater flux is estimated to be 0.552 $\times 10^6$ $m^3 s^{-1}$ (Pickard and Emery 1990, Fig. 5.9). The model heat flux at the southern sponge is 0.12×10^{14} J s^{-1}, about 10% of the correct value; while the model

salt flux is nearly correct with a value of 1.6×10^7 kg salt s^{-1}, compared with the estimated value of 2.0×10^7 kg salt s^{-1} (using a reference salinity of 35 psu).

The model salt flux is nearly correct, but the model heat flux is only 10% of the correct value. This lack of consistency between model fluxes and estimates requires further analysis. Since there are three basic water conversions occuring in the sponge [near-surface equatorial waters, subtropical mode (Central) waters, and North Atlantic Deep Water to Antarctic Bottom Water], it is convenient to calculate the net flux over three regions of the T–S diagram as indicated in Table 3. These three regions include all of the flux across the outer edge of the sponge. The largest flux is due to the middle class, which is the northward motion of South Atlantic Central Water giving rise to a northward total transport along with northward flux of heat and salt. The next largest contributor to the flux is the coldest class, which combines the northward movement of Antarctic waters and the southward flow of North Atlantic Deep Water giving rise to net southward volume, heat, and salt fluxes. The smallest flux is due to the warm, salty class, which represents the transport of waters near the surface and of equatorial origin giving rise to a southward volume, heat, and salt fluxes.

Fu (1981) estimated the transport of various water masses across 30°S from an inverse calculation. Even though this is farther south than the edge of the sponge, it gives some indication of the volumes for comparison with Table 3. The range of values given here are for two different hydrographic sections for which the inverse calculation was made. The warm surface waters and Antarctic Intermediate Water are estimated to provide a northward transport of 9 to 15 ($\times 10^6$ m^3 s^{-1}) and 6 to 10 ($\times 10^6$ m^3 s^{-1}), respectively. North Atlantic Deep Water has a southward transport of 19 to 22 ($\times 10^6$ m^3 s^{-1}). The most dense water class in Fu's calculation (called Circumpolar Water) has a transport that ranges from 2×10^6 m^3 s^{-1} north to 4×10^6 m^3 s^{-1} south.

The behavior of the sponge layer is clearly wrong for the warmest water class as the model produces 2×10^6 m^3 s^{-1} southward but the inverse calculation indicates 9 to 15 ($\times 10^6$ m^3 s^{-1}) northward. The inadequate northward heat flux means that the warm branch of the global overturning cell is not adequately represented in this simulation. The Central Waters, which correspond to the density range labeled "Antarctic Intermediate Water" in Fu (1981), have an estimated northward transport of 6 to 10 ($\times 10^6$ m^3 s^{-1}), close to the model transport of 6×10^6 m^3 s^{-1}. The third class of water in the model is mainly North Atlantic Deep Water with a small contribution from the Antarctic Bottom Water; the model transport is 3.8×10^6 m^3 s^{-1}, while the inverse derived transport is 19 to 22 ($\times 10^6$ m^3 s^{-1}). The small value of the heat flux from the sponge layer comes from the inadequate production of warm surface water. The flux of North Atlantic Deep Water into the sponge is about 20% of the correct value; if it were closer to the correct value, the southward heat flux would have been even more in error.

d. Labrador influences

The boundary sponge in the northwestern corner of the model represents the processes in Baffin Bay and the Labrador Sea, which produce cold and relatively fresh waters. The exchange across the sponge is 9.3×10^6 m^3 s^{-1} (Table 2) and there is a net cooling and freshening of the water, as expected. The largest transport into the sponge is around 4.0°C and 34.8 psu (Fig. 12b) and the outflow is around 0.0°C and between 33.0 and 34.0 psu (Fig. 12a). The flow near the sponge (Fig. 13a) indicates that Arctic waters enter the sponge along the northern side (64°N) and near the center (61°N). Cold, fresh waters are extruded along the southern side (59° and 60.5°N). However, the circulation is strongly barotropic and there is a certain amount of recirculation (laterally banded flow) in the center of the Labrador Sea.

Estimates of the production of Labrador Sea water are 2.0 to 4.0 ($\times 10^6$ m^3 s^{-1}) (Worthington 1981), 3.9×10^6 m^3 s^{-1} (Clarke and Gascard 1983), and 8.6×10^6 m^3 s^{-1} (McCartney and Talley 1984). Speer and Tziperman (1992) estimate the total production of subpolar mode water to be 14×10^6 m^3 s^{-1}, which accounts for Labrador Sea water production along with other waters. The estimate by Clarke and Gascard (1983) may be the most reliable, in which case the model is producing about twice the proper amount of Labrador Sea Water. The sponge is also producing cold, low salinity Baffin Bay Water, and it is not clear how this is being accounted for in the Labrador Sea estimates referenced above. This mode water production is driven by a heat loss of 0.21×10^{14} J s^{-1} (McCartney and Talley 1984), which matches well with the heat flux from the sponge. Finally, McCartney and Talley (1984) estimate a freshwater flux to the Labrador Sea, consistent with the volume exchanges in their box model, of 0.188×10^6 m^3 s^{-1} or 6.76×10^6 kg salt s^{-1}, a factor of 5 larger than the value obtained from the sponge layer.

e. Mediterranean influences

The final sponge boundary layer between Spain and Morroco is included to provide the warm and salty water created by the Mediterranean Sea. The total exchange across this sponge is 8.5×10^6 m^3 s^{-1} with a net increase in temperature and salinity (Table 2) as would be expected for Mediterranean-derived water. The exchange across this layer is much larger than the Mediterranean outflow of 1.1×10^6 m^3 s^{-1} (Tchernia 1980) or 1.5×10^6 m^3 s^{-1} (Ochoa and Bray 1991). However, an unknown part of the transport across the

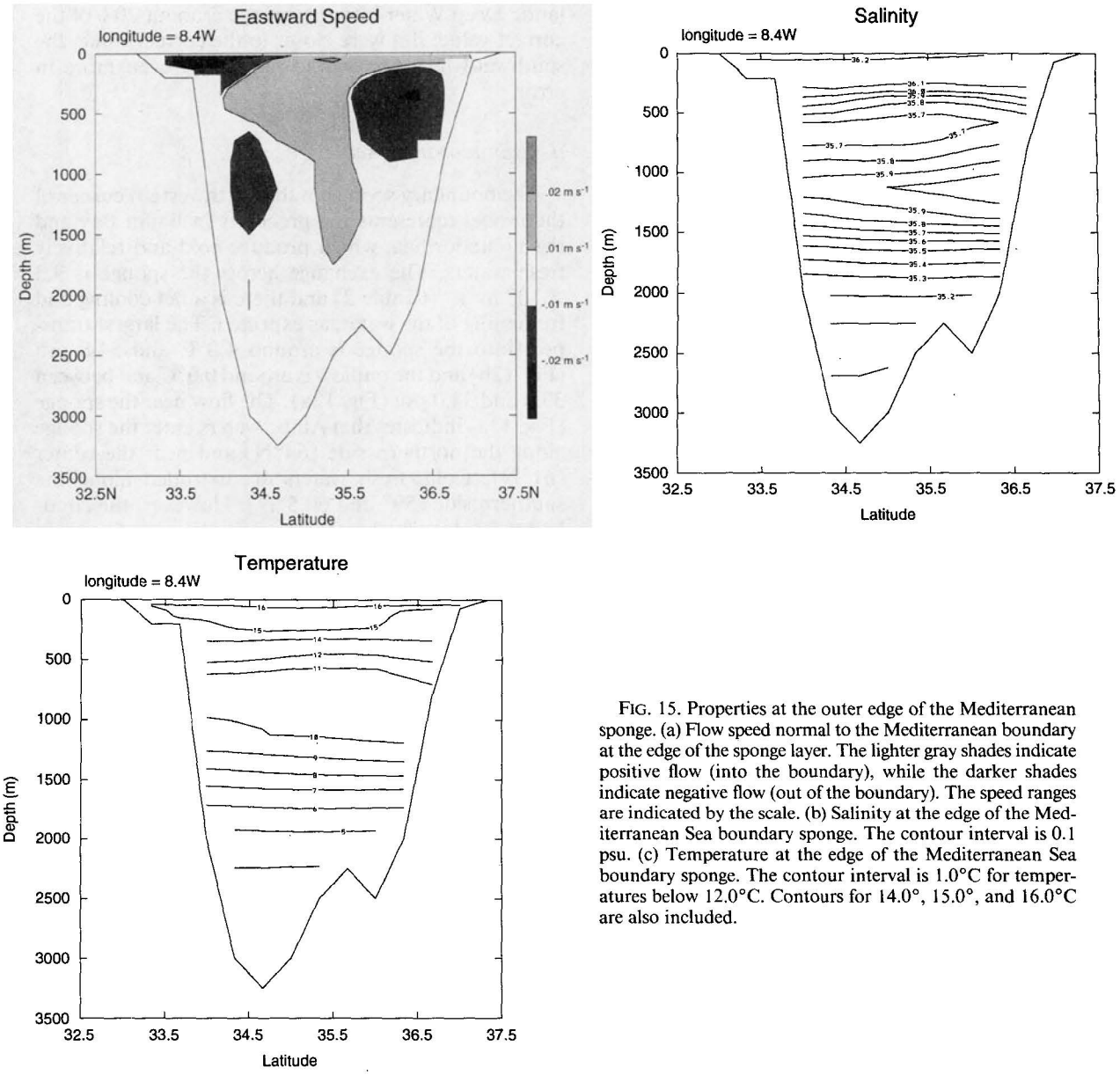

FIG. 15. Properties at the outer edge of the Mediterranean sponge. (a) Flow speed normal to the Mediterranean boundary at the edge of the sponge layer. The lighter gray shades indicate positive flow (into the boundary), while the darker shades indicate negative flow (out of the boundary). The speed ranges are indicated by the scale. (b) Salinity at the edge of the Mediterranean Sea boundary sponge. The contour interval is 0.1 psu. (c) Temperature at the edge of the Mediterranean Sea boundary sponge. The contour interval is 1.0°C for temperatures below 12.0°C. Contours for 14.0°, 15.0°, and 16.0°C are also included.

sponge is associated with the Canary Current, evident as the strong westward flow in the upper 300 m on the southern side of the boundary layer (Fig. 15a).

There is no clear pattern to the water flux by T–S class (Fig. 14a,b), but North Atlantic Central Water is crossing the outer boundary of the sponge. In addition, there is a relatively large outflow at 11.0°C and 35.7 psu, which is a little warm but otherwise about right for Mediterranean Water (Table 1) away from the Strait of Gibralter. The flow pattern at the boundary of the sponge is a little peculiar with eastward flow in the center of the section down to about 1000 m and westward flow on the north side of the sponge at about 500 m and on the south side at about 1000 m. The flow away from the sponge on the northern side represents that part of the Mediterranean outflow that hugs the European coast on its way into the Atlantic or to the Arctic; the southern flow is that part that extends across the southern limb of the subtropical gyre. These circulation patterns seem realistic, but the model inflow to the Mediterranean is spread over a thicker layer than the 400 m indicated in Tchernia (1980, Fig. 5.27) or Ochoa and Bray (1991, Fig. 3). The subsurface salinity maximum occurs at 1400 m (Fig. 15a), but flow speed at this depth is less than 1 mm s^{-1}.

The Mediterranean Sea creates salty water by net evaporation in an amount estimated to be 0.53 m per year (Ochoa and Bray 1991), equivalent to a freshwater

TABLE 3. Volume, heat, and salt flux by temperature and salinity ranges for the southern sponge layer. These three classes represent near-surface equatorial waters, subtropical mode (Central) waters, and North Atlantic Deep Water to Antarctic Bottom Water. These three classes include all of the water crossing the boundary of the sponge.

Salinity (psu)	Temperature (°C)	Volume (Sv)	Heat ($J\ s^{-1}$)	Salt (kg salt s^{-1})
35–38	20–32	1.9 (S)	2.0×10^{14} (S)	6.6×10^{7} (S)
34–38	5–20	6.0 (N)	2.9×10^{14} (N)	37.0×10^{7} (N)
34–35	0–5	3.8 (S)	0.74×10^{14} (S)	13.7×10^{7} (S)

flux into the Mediterranean of 0.042×10^6 $m^3\ s^{-1}$ and implying a salt flux of 3.4 to 4.2 $\times 10^6$ kg salt s^{-1}. However, the salt flux calculated across the sponge (Table 2) is smaller than this estimate by a factor of about 400. The heat flux is estimated to be 0.055 to 0.15 ($\times 10^{14}$ J s^{-1}) (Ochoa and Bray 1991), two to five times the model flux. Since the temperature and salinity structure for this region is generally correct, the insufficient salt flux is due to the circulation, which does not have the deep outflow on the northern side of the sponge. Furthermore, the flow across the sponge is very weak and the depth of the outflow does not match the depth of the salinity maximum, so there is insufficient exchange created by the sponge.

f. Flow in sponges

To understand the reasons for the inadequate performance of the sponge boundary layers, it is worthwhile to consider the dynamics in the sponges. The essence of the boundary condition is that the temperature and salinity of the water in the sponges is driven to a particular value. This imposed structure controls the density and, therefore, the geostrophic shear in the sponge. Assuming that the flow is basically geostrophic, which is an assumption in large-scale dynamics, then the circulation pattern across the boundary of the sponge is determined.

In many cases, the sponge boundary is required to represent part of the thermohaline circulation, so there must be vertical exchanges of water in the sponge. For example, the southern sponge must convert some amount of North Atlantic Deep Water, which moves south at around 3000 m into Antarctic Intermediate Water, that moves north along the western boundary at around 1000 m. In the ocean, such vertical exchange is driven by vertical convection or subduction along density surfaces. Both of these processes must be simulated in the narrow sponge layer. Vertical exchange in the sponge can occur by only two methods: directly driven by source-sink flow or convective mixing.

The first method is basically a kinematic condition that if water enters the sponge in the upper layers and exits in the lower layers, then conservation of volume requires vertical motion. However, in a rotating fluid, there are dynamical penalties for strong vertical motion that are mainly the creation of relative vorticity. This vertical motion can also cause modification of potential energy, but recall that the sponge is changing the temperature and salinity of the water being moved vertically, so slow motion will not involve potential energy changes within the sponge.

Two estimates for the required vertical velocity in the sponge are as follows. Consider the conversion of North Atlantic Deep Water into Antarctic Intermediate Water in the southern sponge and Atlantic Surface Water into Mediterranean Water in the Mediterranean sponge. An estimate of the vertical velocity for these cases requires only the volume flux being converted, the width of the sponge layer and the horizontal distance over which the vertical flow occurs. In the first case, the flux of Antarctic Intermediate Water out of the southern sponge is about 10×10^6 $m^3\ s^{-1}$. The sponge has a width of 5/3° latitude (5 grid intervals), and the estimated horizontal extent of the northward flow is 5° longitude (Fig. 11a). These conditions require a vertical velocity of about 1.0×10^{-4} m s^{-1}. The largest vertical velocity in the sponge from the 5-year average solution is about one-quarter of this value (figure not shown). The second case converts 1.2×10^6 $m^3\ s^{-1}$ of Atlantic surface water into Mediterranean Water in a sponge that is 2° longitude wide and has a horizontal extent of 2.5° latitude (Fig. 15). The required vertical velocity is 2.4×10^{-5} m s^{-1}.

The estimated vertical velocity for large-scale circulation is $W = \epsilon UH/L$, where ϵ (= 0.001) is the Rossby number, U (= 0.1 m s^{-1}) is the flow speed, H (=5 km) is the vertical scale, and L (=1000 km) is the horizontal scale. The vertical velocity scale is, thus, 5.0×10^{-6} m s^{-1}, which is one to two orders of magnitude smaller than the estimated vertical velocity in the sponge. This presumes that the dynamics in the sponge are geostrophic, which is not exactly true, but it does indicate the size of the vertical velocity that is consistent with the dynamics of large-scale flow. If the sponges are made wider than the five grid intervals used in the CME, then the estimated vertical velocities would be smaller. Sponge layers would have to be 50 grid points wide to reduce the required vertical velocity by an order of magnitude, clearly not a practical change in the model. Note in passing that the required vertical velocities are not so large as to violate the requirement of hydrostatic balance in the vertical.

The second method for vertical exchange of water is convective adjustment, imposed in the model as an ad hoc procedure. If the density of a water column is statically unstable, then convection is imposed by simply mixing the water column vertically. This procedure is a very efficient way to carry water vertically. However, not every sponge layer will produce convective instability. The northern and Labrador sponges have the possibility of creating unstable water masses since they cool the incoming water from the surface of the

North Atlantic. Note, however, that since the Levitus temperature and salinity result in a statically stable water column, it is only the transient conditions that give rise to the possibility of vertical convection. The conditions in the southern and Mediterranean sponges will not lead to convection because of warm surface waters in the southern sponge and salty deep waters in the Mediterranean sponge.

6. Summary

A T–S volumetric census, with a resolution of 0.2°C and 0.1 psu, of years 20–25 of the WOCE Community Modeling Effort, eddy-resolving simulation of the equatorial and North Atlantic Ocean reveals how the thermohaline character of the model has changed from the initial conditions taken from the Levitus (1982) climatology. Since there are no internal sources or sinks of heat or salt in the model, any changes, other than internal mixing, must be due to the boundary conditions. These conditions are imposed at the surface and at four sponge layers at the northern boundary, southern boundary, Labrador Sea, and Mediterranean Sea, where water temperature and salinity are nudged toward climatological conditions.

Several unrealistic thermohaline features appear in the solution, which can be traced to these surface and lateral sponge boundary conditions.

All of the water masses created in the Arctic Ocean have volumes in the model that are too large. The volume transport across the northern sponge is twice the value estimated from observations. The heat flux is approximately correct, while the salt flux is too large by a factor of 4. Water masses created in the South Atlantic occur in volumes that are smaller than observed. The transport of water across the southern sponge is about two-thirds of the observed value, but the salt flux is comparable with estimates. However, the heat flux is only 10% of the measured values due to a missing equatorward motion of warm surface waters. Water masses created in the Labrador Sea and Baffin Bay occur in volumes that are larger than indicated by the climatology. The volume flux is twice the observed value, while the heat flux from the sponge is realistic. The salt flux is about 20% of the observed value. Finally, Mediterranean Water occurs in volumes that are too small. Even though the volume transport across the sponge boundary is high by a factor of 8, the net salt flux is small by a factor of 400, leading to an insufficient production of salt.

All of these difficulties with the model T–S structure are traced to three general problems. First, the flow at the outer edge of the sponges is strongly barotropic in spite of the fact that the temperature and salinity fields are from climatology. Part of the problem with the sponges may be the smoothed nature of the climatology, which has the effect of reducing density gradients, thereby reducing the geostrophic shears. In all cases, except the southern sponge, the volume transport across the sponge is two to eight times larger than the value expected by the climatology. Since the vertical structure of the flow is set by the climatology, the only way for the flow to create this additional transport is through barotropic flow. The reason for the additional transport is not entirely clear, but it may be due to the excessive vertical velocities demanded by the conversion process. These vertical motions create bound vortices in the sponge layers that drive recirculation in the vicinity of the sponges, increasing the transport without changing the heat or salt flux.

The second problem is that some of the sponges do not work well because of geometric effects. One such problem is that Iceland blocks the flow along the northern sponge so that the water that enters on the eastern side of Iceland cannot exit on the western side. A second problem is that the true ocean depth is used in the sponge layers. In the inner part of the Mediterranean sponge where the relaxation time is the smallest, the water is so shallow (around 100 m) that there is very little volume in which to modify the water. Since there is no source of water in the sponge, there is very little exchange of water with different character. A similar problem occurs in the Labrador sponge where the water is only 100 m deep.

The third general problem is the use of relaxation to climatology to represent surface freshwater fluxes, which leads to unrealistic surface forcing if the currents are displaced from climatological locations. The combination of a displaced Gulf Stream and the relaxation of surface salinity to climatology produces mode waters that are unrealistically cool and fresh.

Acknowledgments. I would like to thank Bill Holland and Frank Bryan for all of their efforts in running this extended simulation. Additionally, Frank Bryan was very helpful in providing information about the model code, forcing, and solution from the various files stored at NCAR. Finally, I would like to acknowledge the National Center for Atmospheric Research, which is sponsored by the National Science Foundation, for the use of its computers and file storage system. Various individuals in the Scientific Computing Division of NCAR, notably Steve Worley, were very helpful at various stages in this project. This work is part of the U.S. contribution to International WOCE and has been supported by funds from the National Science Foundation under Grant OCE-89-22860.

REFERENCES

Bryan, K., 1969: A numerical method for the study of the circulation of the World Ocean. *J. Comput. Phys.*, **4**, 347–376.

——, and W. R. Holland, 1989: A high resolution simulation of the wind- and thermohaline-driven circulation of the North Atlantic Ocean. *Parameterization of small scale processes,* Proc. *'Aha Huliko'a, Hawaiian Winter Workshop,* University of Hawaii at Manoa, 99–115.

Clarke, R. A., and J.-C. Gascard, 1983: The formation of Labrador Sea Water. Part I: Large-scale processes. *J. Phys. Oceanogr.*, **13,** 1764–1778.

Dickson, R. R., E. M. Gmitrowicz, and A. J. Watson, 1990: Deep-water renewal in the northern North Atlantic. *Nature,* **344,** 848–850.

Fu, L.-L., 1981: The general circulation and meridional heat transport of the subtropical South Atlantic determined by inverse methods. *J. Phys. Oceanogr.*, **11,** 1171–1192.

Han, Y. J., 1984: A numerical world ocean circulation model. Part II: A baroclinic experiment. *Dyn. Atmos. Oceans,* **8,** 141–172.

Hastenrath, S., 1982: On meridional heat transport in the World Ocean. *J. Phys. Oceanogr.*, **12,** 922–927.

Hellerman, S., and M. Rosenstein, 1983: Normal monthly wind stress over the world ocean with error estimates. *J. Phys. Oceanogr.*, **13,** 1093–1104.

Hsiung, J., 1985: Estimates of global oceanic meridional heat transport. *J. Phys. Oceanogr.*, **15,** 1405–1413.

Klinck, J. M., 1994: Thermohaline structure of the CME. *WOCE Notes,* **6**(2), 4–8.

Levitus, S., 1982: *Climatological Atlas of the World Ocean.* NOAA Prof. Paper 13, U.S. Govt. Printing Office, 173 pp.

McCartney, M. S., and L. D. Talley, 1982: The subpolar mode water of the North Atlantic Ocean. *J. Phys. Oceanogr.*, **12,** 1169–1188.

——, and ——, 1984: Warm-to-cold water conversion in the northern North Atlantic Ocean. *J. Phys. Oceanogr.*, **14,** 922–935.

Mesinger, F., and A. Arakawa, 1976: *Numerical Methods Used in Atmospheric Models.* Vol. I, GARP Publication Series, No. 17, 64 pp.

Ochoa, J., and N. A. Bray, 1991: Water mass exchange in the Gulf of Cadiz. *Deep-Sea Res.*, **38** (Suppl. 1), S465–S503.

Pickard, G. L., and W. J. Emery, 1990: *Descriptive Physical Oceanography: An Introduction. 5th ed.* Pergamon Press, 320 pp.

Schott, F. A., and C. Böning, 1991: Evaluation of the WOCE model in the western equatorial Atlantic: Upper layer circulation. *J. Geophys. Res.*, **96,** 6993–7004.

Spall, M. A., 1990: Circulation in the Canary Basin: A model/data analysis. *J. Geophys. Res.*, **95,** 9611–9628.

——, 1992: Rossby wave radiation in the Cape Verde Frontal Zone. *J. Phys. Oceanogr.*, **22,** 796–807.

Speer, K., and E. Tziperman, 1992: Rates of water mass formation in the North Atlantic Ocean. *J. Phys. Oceanogr.*, **22,** 93–104.

Swift, J. H., 1986: The arctic waters. *The North Sea,* B. G. Hurdle, Ed., Springer-Verlag, 129–154.

Tchernia, P., 1980: *Descriptive Regional Oceanography.* Pergamon Press, 253 pp.

Treguier, A. M., 1992: Kinetic energy analysis of an eddy resolving, primitive equation North Atlantic model. *J. Geophys. Res.*, **97,** 687–701.

Warren, B. A., 1972: Insensitivity of subtropical mode water characteristics to meteorological fluctuations. *Deep-Sea Res.*, **19,** 1–19.

Worthington, L. V., 1959: The 18° Water in the Sargasso Sea. *Deep-Sea Res.*, **5,** 297–305.

——, 1981: The water masses of the World Ocean: Some results of a fine-scale census. *Evolution of Physical Oceanography,* B. A. Warren and C. Wunsch, Eds., The MIT Press, 42–69.

Wüst, G., 1964: *Stratification and Circulation in the Antillean–Caribbean Basins.* Columbia University Press, 54 pp.